THE DEUTERON D-STATE AND (d,p) REACTIONS

George Delic

A thesis submitted for the
degree of Doctor of Philosophy
at the Australian National University
Canberra

November 1970

To my Parents

This thesis is based on a series of papers which have been (or shortly will be) published in the journal 'Nuclear Physics' as follows:

"Effect of tensor forces in the deuteron-nucleus interaction on DWBA calculations for (d,p) reactions."

volume A127 (1969) p.234,

"j-dependence in ℓ = 1 transitions in Cr(d,p) reactions."

volume A134 (1969) p.470,

"DWBA calculations for (d,p) reactions including the D-state of the deuteron."

accepted for publication,

"Effect of the deuteron D-state on DWBA calculations for $^{16}O(p,d)^{15}O$ and $^{40}Ca(d,p)^{41}Ca$."

accepted for publication,

the first three are co-authored with Dr. B.A. Robson and the last is the candidate's own work. Chapter 1 contains more details of the theory than given in these papers.

No part of this thesis has been presented for a degree at any other university.

George Dehnic

23/11/70

I wish to acknowledge a great debt of gratitude to my supervisor, Dr. B.A. Robson, for his patient guidance and many valuable discussions throughout the course of these studies.

I also wish to thank Professor K.J. Le Couteur for his helpful encouragement, and Drs. C.A. Edvi-Illes and R.S. Mackintosh for reading the manuscript and their useful suggestions.

George Delic

ABSTRACT

The zero-range formulation of the DWBA theory for deuteron stripping has been used to describe qualitatively the j-dependence of several $\ell = 1$ transitions in $^{50,52}Cr(d,p)$ reactions at 7.5 and 8.0 MeV deuteron bombarding energy. This description required a different deuteron potential from that obtained by fitting elastic scattering data implying that the DWBA theory is not strictly valid. The transition to the 1.895 MeV level in ^{51}Cr was found to violate the j-dependence rule of Lee and Schiffer. The effect of possible tensor forces in the deuteron-nucleus interaction on similar calculations has been studied for $\ell = 1$ transitions in the $^{40}Ca(d,p)^{41}Ca$ reaction leading to the 2.47 MeV ($\frac{3}{2}^-$) and 3.95 MeV ($\frac{1}{2}^-$) levels. In particular the j-dependence of the cross sections and vector analysing powers has been investigated. The D-state of the deuteron has been included in an exact finite-range treatment using a soft core neutron-proton potential and the corresponding deuteron bound-state wave function of Reid. The effect of the D-state upon the j-dependence of the differential cross sections and the corresponding vector and tensor analysing powers has been investigated for $\ell = 1$ transitions in $^{52}Cr(d,p)$, $^{40}Ca(d,p)$ and $^{16}O(p,d)^{15}O$ reactions.

CONTENTS

INTRODUCTION

In recent years the Distorted Wave Born Approximation (DWBA) theory (see for example the bibliography and references given by Tobocman[1])) has been widely used in the analysis of neutron transfer reactions initiated by low energy deuterons or protons. The formulations of this theory usually involve the so called "zero-range (ZR) approximation" and assume a purely S-state deuteron. This thesis discusses some DWBA optical model (OM) analyses with and without these two approximations.

The ZR form of the DWBA theory has been repeated in detail in section 1.2 as a prelude to the full finite-range (FR) treatment of section 1.3 which also includes the deuteron D-state. Calculations based on this formulation are discussed in chapter 4.

In chapter 2 a theoretical study was carried out of an empirically observed phenomenon which has been termed "j-dependence" (see section 2.1), and an attempt was made to evaluate the usefulness of a DWBA analysis in its description.

It has been shown[2]) that there are three possible tensor terms which may be included in the deuteron-nucleus OM potential. The effect of two of these tensor terms was investigated in chapter 3 and calculations have been performed for some typical examples of $\ell = 1$ transitions in a (d,p) reaction on a 2p-shell nucleus.

CHAPTER 1

THEORY OF DWBA FOR (d,p) REACTIONS

1.1 Introduction

The usual DW amplitude[3]) for a (d,p) reaction contains the factor $D(\underline{r}_d) = V_{pn}(\underline{r}_d)\phi_d(\underline{r}_d)$ which is the product of the neutron-proton potential and the internal wave function of the deuteron. In previous calculations two approximations have generally been made: (i) ϕ_d is assumed to be entirely S-state and (ii) $D(\underline{r}_d)$ is replaced by $D_0\delta(\underline{r}_d)$, the so called "zero-range approximation". In a few cases[4-6]) the second approximation has been relaxed with $D(\underline{r}_d)$ set equal to a "finite-range function", usually of a Gaussian form, $D_G\exp(-r_d^2/R_G^2)$, with D_G and R_G adjusted so that the Fourier transform of $D(\underline{r}_d)$ has the same zero and small momentum components as the ZR form factor for a suitably normalized deuteron wave function (e.g. Hulthén wave function). The introduction of a FR form factor requires the evaluation of six-dimensional integrals compared with the three-dimensional integrals of the ZR calculations. Consequently, several authors[7-9]) have proposed an approximate treatment of FR effects, the "local energy approximation", which involves only a simple radial correction factor in the usual ZR formalism. The accuracy of this approximation has been verified by comparison with exact (Gaussian form factor) FR calculations for the differential cross sections. Using a

similar FR approximation, the D-state of the deuteron has been included in DW calculations by Johnson and Santos[10,11]) and was found to have a large effect on the angular distributions for orbital angular momentum transfers of $\ell = 3$. Pearson[12,13]) uses a similar approximate treatment to include the D-state in the "weakly bound particle" model. Apart from these studies, the D-state has been neglected in all previous calculations.

Section 1.3 presents a formulation of the DWBA theory for (d,p) reactions which gives an exact account of the deuteron D-state. This treatment is "exact" in the sense that FR DWBA calculations were then performed using a deuteron bound-state solution of Reid[14]). However possible distortion of this wave function in the vicinity of the nuclear surface and subsequent deuteron break-up were ignored.

Prior to the full FR treatment, the well known ZR result[15]) is derived in the next section.

1.2 Zero-range formulation

This section presents a formulation of the ZR DWBA theory of deuteron induced stripping reactions. The following definitions are used:

i) r_{ab} is the separation distance of the centres-of-mass of particles a and b,

ii) Ω_{ab} are the angular coordinates of $\underline{r}_{ab}$,

iii) r_c and Ω_c are the "internal" coordinates (corresponding to

i) and ii)) of particle c,

iv) $M_{aA} = \frac{m_a M_A}{M_A + m_a}$ is the reduced mass for particles a, A,

v) I_c is the spin (with component μ_c) of particle c.

The DWBA transition amplitude for the reaction T(d,p)R is given by[16])(see also ref.[17,18]))

$$R(\mu_d\mu_T\to\mu_p\mu_R) = -\frac{M_{pR}}{2\pi\hbar^2}\int \Psi_p(r'_{pR},\pi-\theta,\mu_p)\phi_R^{\dagger}(\underline{r}_R,\mu_R)V_{np}(\underline{r}_d)\Psi(\underline{r}_d,\underline{r}_{dT},\mu_d)$$

$$\cdot\phi_T(\underline{r}_T,\mu_T)d\underline{r}_R d\underline{r}'_{pR} \qquad (1.1)$$

$\Psi_p(r'_{pR},\pi-\theta,\mu_p)$ is related to the elastic scattering wave function which itself is a solution of a homogeneous differential equation for the asymptotic condition (in the absence of Coulomb effects) of a plane wave plus an outgoing spherical wave (see Mott and Massey[18])). Henceforward, for the sake of simplicity, the prime on the coordinate $\underline{r}'_{pR}$ is omitted.

V_{np} is the neutron-proton interaction, assumed here to be a central, spin-independent potential. The wave function $\Psi(\underline{r}_d,\underline{r}_{dT},\mu_d)$ can be factorized into two terms: a function $\phi_d(\underline{r}_d)$ representing the radial and angular parts of the internal deuteron wave function for the ground state, neglecting the D-state component, and $\Psi_d(\underline{r}_{dT},\mu_d)$ representing the elastic scattering wave function for an incident beam of deuterons in a spin state μ_d scattered by a spin-dependent optical potential, i.e.

$$\Psi(\underline{r}_d,\underline{r}_{dT},\mu_d) = \phi_d(\underline{r}_d)\Psi_d(\underline{r}_{dT},\mu_d)$$

and Ψ_d satisfies the appropriate asymptotic condition (see eqn. (1.12)).

Assuming that the optical potentials in both channels have spin-orbit terms, the proton and deuteron distorted waves may be written explicity as[16,17])

$$\Psi_p(r_{pR},\pi-\theta,\mu_p) = \sum_{J_p L_p M_p} 4\pi i^{-L_p} Y_{L_p}^{M_p}(\Omega_{k_p})\, C(L_p\,\tfrac{1}{2}\,J_p, M_p\mu_p M_p+\mu_p)$$

$$\cdot \sum_{\mu_p'} C(L_p\,\tfrac{1}{2}\,J_p, M_p+\mu_p-\mu_p'\,\mu_p'\,M_p+\mu_p)\, Y_{L_p}^{M_p+\mu_p-\mu_p'}(\Omega_{pR})^*$$

$$\cdot R_{J_p L_p}(r_{pR})\chi_{\frac{1}{2}}^{\mu_p'\,\dagger} \qquad (1.2)$$

and

$$\Psi(\underline{r}_d,\underline{r}_{dT},\mu_d) = \phi_d(\underline{r}_d) \sum_{J_d L_d L_d' M_d} 4\pi i^{L_d} Y_{L_d}^{M_d}(\Omega_{k_d})^*\, C(L_d\,1\,J_d, M_d\mu_d M_d+\mu_d)$$

$$\cdot \sum_{\mu_d'} C(L_d'\,1\,J_d, M_d+\mu_d-\mu_d'\,\mu_d'\,M_d+\mu_d)$$

$$\cdot Y_{L_d'}^{M_d+\mu_d-\mu_d'}(\Omega_{dT})\, R_{J_d L_d L_d'}(r_{dT})\chi_1^{\mu_d'} \qquad (1.3)$$

where $C(j_1 j_2 j_3, m_1 m_2 m_3)$ is the Clebsch-Gordan coefficient as defined by Rose[19]). For the proton, Ω_{k_p} refers to the momentum $\underline{k}_p$ along the outgoing direction, J_p is the total angular momentum with component $M_p + \mu_p$ and L_p the orbital angular momentum. For

the deuteron, Ω_{k_d} refers to the momentum $\underline{k}_d$ along the incoming direction, J_d is the total angular momentum with component $M_d + \mu_d$ and L_d and L_d' the incoming and outgoing orbital angular momenta respectively. $R_{J_p L_p}(r_{pR})$ and $R_{J_d L_d L_d'}(r_{dT})$ are the corresponding radial wave functions, and the symbols Y and χ, as usual, represent angle and spin functions. In eqn.(1.1) $\phi_T(\underline{r}_T, \mu_T)$ is the internal wave function for the ground state of the target (or core) and that for the residual nucleus, $\phi_R(\underline{r}_R, \mu_R)$ may be written as

$$\phi_R(\underline{r}_R, \mu_R) = \phi_R(\underline{r}_T, \underline{r}_{nT}, \mu_R)$$

This wave function is expressed as a sum over the various states of the captured neutron about the target nucleus core. If the "reduced width amplitude"[20]) $\theta^*_{j\ell}$ is a measure of the probability of capturing the neutron into a particular state of orbital angular momentum ℓ (component m) and total angular momentum j, then

$$\phi_R^\dagger(\underline{r}_T, \underline{r}_{nT}, \mu_R) = \sum_{j\ell m} C(I_T j I_R, \mu_T\ \mu_j \mu_R) \cdot C(\ell \tfrac{1}{2} j, m\ \mu_n \mu_j)\theta^*_{j\ell} u_{j\ell}(r_{nT}) \cdot i^{-\ell} Y_\ell^m(\Omega_{nT})^* \chi_{\frac{1}{2}}^{\mu_n \dagger} \phi_T^\dagger(\underline{r}_T, \mu_T) \qquad (1.4)$$

where $\mu_j = \mu_R - \mu_T$, and $u_{j\ell}(r_{nT})$ is the radial part of the neutron bound-state wave function. Substituting eqn.(1.4) into (1.1), the integral over $\underline{r}_R$ can be replaced by integrals over $\underline{r}_T$ and $\underline{r}_{nT}$.

If

$$\int \phi_T^{\dagger}(\underline{r}_T,\mu_T)\phi_T(\underline{r}_T,\mu_T)d\underline{r}_T = 1$$

then eqn.(1.1) becomes:

$$R(\mu_d\mu_T\rightarrow\mu_p\mu_R) = -\frac{M_{pR}}{2\pi\hbar^2}\sum_{j\ell m} i^{-\ell}\theta^*_{j\ell}\, C(I_T j I_R,\mu_T\mu_j\mu_R)$$

$$\cdot\, C(\ell\tfrac{1}{2}j,m\ \mu_j-m\ \mu_j)\chi^{\mu_j-m\dagger}_{1/2}$$

$$\cdot \int \Psi_p(r_{pR},\pi-\Theta,\mu_p)u_{j\ell}(r_{nT})Y^m_\ell(\Omega_{nT})^*$$

$$\cdot V_{np}(\underline{r}_d)\ \Psi(\underline{r}_d,\underline{r}_{dT},\mu_d)d\underline{r}_{nT}\ d\underline{r}_{pR} \qquad (1.5)$$

The expansions (1.2) and (1.3) may then be substituted into eqn.(1.5). Noting that

$$\chi^{\mu'_d}_1 = \sum_{\bar{\mu}_p} C(\tfrac{1}{2}\tfrac{1}{2}1,\mu_n\bar{\mu}_p\mu'_d)\chi^{\mu_n}_{1/2}\chi^{\bar{\mu}_p}_{1/2}$$

then

$$\chi^{\mu'_p\dagger}_{1/2}\chi^{\bar{\mu}_p}_{1/2} = \delta_{\mu'_p,\,\bar{\mu}_p}$$

$$\chi^{\mu_j-m\dagger}_{1/2}\chi^{\mu'_d-\mu'_p}_{1/2} = \delta_{\mu_j-m,\mu'_d-\mu'_p}$$

and $m = \mu_j+\mu'_p-\mu'_d$

Consequently the elements of the transition matrix are given by

$$R(\mu_d\mu_T\to\mu_p\mu_R) = -\frac{M_{pR}}{2\pi\hbar^2}\sum_{\substack{J_dJ_pL_dL'_dL_pj\ell\\ M_dM_p\mu'_d\mu'_p}}(4\pi)^2\, i^{L_d-L_p-\ell}\,\theta^*_{j\ell}$$

$$\cdot\, Y^{M_p}_{L_p}(\Omega_{k_p})\; Y^{M_d}_{L_d}(\Omega_{k_d})^*\; C(I_TjI_R,\mu_T\mu_j\mu_R)$$

$$\cdot\, C(\ell\tfrac{1}{2}j,\mu_j+\mu'_p-\mu'_d\;\mu'_d-\mu'_p\;\mu_j)\; C(\tfrac{1}{2}\tfrac{1}{2}1,\mu'_d-\mu'_p\;\mu'_p\;\mu'_d)$$

$$\cdot\, C(L_p\tfrac{1}{2}J_p,M_p\mu_pM_p+\mu_p)\; C(L_p\tfrac{1}{2}J_p,M_p+\mu_p-\mu'_p\;\mu'_p\;M_p+\mu_p)$$

$$\cdot\, C(L_d1J_d,M_d\mu_dM_d+\mu_d)\; C(L'_d1J_d,M_d+\mu_d-\mu'_d\;\mu'_d\;M_d+\mu_d)$$

$$\cdot\, \mathcal{J} \qquad (1.6)$$

where

$$\mathcal{J} = \int R_{J_pL_p}(r_{pR})R_{J_dL_dL'_d}(r_{dT})u_{j\ell}(r_{nT})V_{np}(\underline{r}_d)\phi_d(\underline{r}_d)$$

$$\cdot\, Y^{M_p+\mu_p-\mu'_p}_{L_p}(\Omega_{pR})^*\; Y^{M_d+\mu_d-\mu'_d}_{L'_d}(\Omega_{dT})\; Y^{m}_{\ell}(\Omega_{nT})^*\; d\underline{r}_{nT}d\underline{r}_{pR}$$

At this stage the ZR approximation may be introduced to reduce the six-dimensional integral to one over three dimensions. Let

$$V_{np}(\underline{r}_d)\;\phi_d(\underline{r}_d) = D_0\;\delta(\underline{r}_d) \qquad (1.7)$$

also (see Appendix)

$$\underline{r}_d = \underline{r}_{pR} - \frac{M_T}{M_R}\;\underline{r}_{nT}$$

so that[21])

$$\delta(\underline{r}_d) = \delta(\underline{r}_{pR} - \frac{M_T}{M_R}\,\underline{r}_{nT}) \left[\frac{m_d M_R}{m_n(M_T + m_d)}\right]^{-3}$$

changing the variables of integration to $\underline{r}_{dT}$ and $\underline{r}_{pR}$ (see Appendix) introduces a Jacobian J:

$$J = \left[\frac{m_d\, M_R}{m_n\,(M_T + m_d)}\right]^3$$

Then

$$\mathcal{J} = D_0 \int R_{J_p L_p}\left(\frac{M_T}{M_R}\, r_{nT}\right) R_{J_d L_d L'_d}(r_{dT}) u_{j\ell}(r_{nT})$$

$$\cdot\, Y^{M_p+\mu_p-\mu'_p}_{L_p}(\Omega_{nT})^*\; Y^{M_d+\mu_d-\mu'_d}_{L'_d}(\Omega_{dT})\; Y^{m}_{\ell}(\Omega_{nT})^*\; d\underline{r}_{dT}$$

and in ZR $\underline{r}_{nT} = \underline{r}_{dT} = \underline{r}$, whence

$$\mathcal{J} = (-1)^{\mu_j+\mu'_p-\mu'_d} \left[\frac{(2\ell+1)(2L'_d+1)}{4\pi(2L_p+1)}\right]^{1/2} C(\ell L'_d L_p, 000)$$

$$\cdot\, C(\ell L'_d L_p, \mu'_d-\mu'_p-\mu_j\;\; M_d+\mu_d-\mu'_d\;\; M_p+\mu_p-\mu'_p)$$

$$\cdot\, D_0 \int R_{J_p L_p}\left(\frac{M_T}{M_R}\, r\right) R_{J_d L_d L'_d}(r)\; u_{j\ell}(r)\; r^2\, dr$$

and $$M_d = M_p + \mu_p + \mu_j - \mu_d \qquad (1.8)$$

The transition matrix becomes

$$R(\mu_d\mu_T\to\mu_p\mu_R) = -D_o\sqrt{4\pi}\,\frac{2M_pR}{\hbar^2}\sum_{\substack{J_dL_dL'_dM_p\\J_pL_pj\ell}} i^{L_d-L_p-\ell}\,\theta^*_{j\ell}\left[\frac{(2\ell+1)(2L'_d+1)}{(2L_p+1)}\right]^{1/2}$$

$$\cdot\, Y^{M_p}_{L_p}(\Omega_{k_p})\; Y^{M_p+\mu_p+\mu_j-\mu_d}_{L_d}(\Omega_{k_d})^*\; I_{J_pL_pJ_dL_dL'_d\ell j}$$

$$\cdot\, C(I_TjI_R,\mu_T\mu_j\mu_R)\; C(\ell L'_dL_p,000)$$

$$\cdot\, C(L_p\tfrac{1}{2}J_p,M_p\mu_pM_p+\mu_p)\; C(L_dlJ_d,M_p+\mu_p+\mu_j-\mu_d\mu_dM_p+\mu_p+\mu_j)$$

$$\cdot\sum_{\mu'_d\mu'_p}(-1)^{\mu'_p-\mu'_d+\mu_j}\; C(L_p\tfrac{1}{2}J_p,M_p+\mu_p-\mu'_p\mu'_pM_p+\mu_p)$$

$$\cdot\, C(L'_dlJ_d,M_p+\mu_p+\mu_j-\mu'_d\mu'_dM_p+\mu_p+\mu_j)$$

$$\cdot\, C(\ell\tfrac{1}{2}j,\mu_j+\mu'_p-\mu'_d\mu'_d-\mu'_p\mu_j)\,C(\tfrac{1}{2}\tfrac{1}{2}1,\mu'_d-\mu'_p\mu'_p\mu'_d)$$

$$\cdot\, C(\ell L'_dL_p,\mu'_d-\mu'_p-\mu_j\;\; M_p+\mu_p+\mu_j-\mu'_d\;\; M_p+\mu_p-\mu'_p) \qquad (1.9)$$

where

$$I_{J_pL_pJ_dL_dL'_d\ell j} = \int R_{J_pL_p}\left(\frac{M_T}{M_R}\,r\right)\; R_{J_dL_dL'_d}(r)u_{j\ell}(r)r^2dr$$

The summations over μ'_d and μ'_p may then be performed to give the final form of the transition matrix elements as used in the ZR calculations,

$$R(\mu_d\mu_T\to\mu_p\mu_R) = -D_o\sqrt{4\pi}\,\frac{2M_pR}{\hbar^2}\sum_{\substack{J_dL_dL'_dM_p\\J_pL_p\ j\ell}} i^{L_d-L_p-\ell}\,\theta^*_{j\ell}$$

$$\cdot\,(-1)^{\mu_j+L'_d+L_p+J_d+J_p}\,[3(2\ell+1)(2L'_d+1)(2j+1)(2J_d+1)]^{1/2}$$

$$\cdot\,Y^{M_p}_{L_p}(\Omega_{k_p})\;Y^{M_p+\mu_p+\mu_j-\mu_d}_{L_d}(\Omega_{k_d})^*\;I_{J_pL_pJ_dL_dL'_d\ell j}$$

$$\cdot\,C(I_Tj I_R,\mu_T\mu_j\mu_R)\;C(L'_d\;\ell L_p,000)$$

$$\cdot\,C(L_p\,\tfrac{1}{2}J_p,M_p\;\mu_p\;M_p+\mu_p)$$

$$\cdot\,C(L_d\;1\;J_d;\;M_p+\mu_p+\mu_j-\mu_d\;\mu_d\;M_p+\mu_p+\mu_j)$$

$$\cdot\,C(J_d\;j\;J_p,\;M_p+\mu_p+\mu_j,-\mu_j\;M_p+\mu_p)$$

$$\cdot\,X(L_p\,\tfrac{1}{2}J_p,\ell\;\tfrac{1}{2}\;j,\;L'_d\;1\;J_d) \qquad (1.10)$$

where the X coefficient is as defined in ref.[22]).

In the integral $I_{J_pL_pJ_dL_dL'_d\ell j}$ of eqn.(1.10), the radial parts of the proton and deuteron distorted waves are obtained as solutions of radial equations for OM potentials of the form

$$U(r) = C - Vg(V) - i[W_vg(W) + Wf(W)]$$
$$+ (S + iT)r^{-1}[dg(S)/dr]\;\underline{\sigma}\cdot\underline{L}$$
$$+ Mf(R)T_R + Qf(L)T_L\ , \qquad (1.11)$$

where

$$g(i) = \left(1 + \exp[(r - r_i A^{1/3})/a_i]\right)^{-1} ,$$

$$f(i) = 4[g(i)]^2 \exp[(r - r_i A^{1/3})/a_i] ,$$

$$T_R = [(\underline{S} \cdot \underline{r})^2 r^{-2} - \tfrac{2}{3}] ,$$

$$T_L = [(\underline{S} \cdot \underline{L})^2 + \tfrac{1}{2}(\underline{S} \cdot \underline{L}) - \tfrac{2}{3} \underline{L}^2] .$$

C is the Coulomb potential for a uniform charge distribution of radius $R_c = r_c A^{1/3}$ and A the mass number of the nucleus. The neutron bound-state wave functions $u_{j\ell}(r)$ were obtained by adjusting the depth of a real Woods-Saxon potential to give the correct binding energies.

For a deuteron OM potential of the form given in eqn.(1.11) the partial wave expansion of eqn.(1.3) for large values of r satisfies the condition,

$$\Psi_d \sim \left(\left[1 + \frac{\eta^2}{i(kr - \underline{k}.\underline{r})}\right] e^{i(\underline{k}.\underline{r} + \eta \log(kr - \underline{k}.\underline{r}))}\right) \chi_1^{\mu_d}$$

$$+ \sum_{\mu_d'} M_{\mu_d \mu_d'}(\theta,\phi) r^{-1} e^{i(kr - \eta \log 2kr + 2\sigma_0)} \chi_1^{\mu_d'} \qquad (1.12)$$

where $\eta = Ze^2/\hbar v$ and $\sigma_0 = \arg\Gamma(1 + i\eta)$ are the usual Coulomb parameters and $M_{\mu_d \mu_d'}$ the elastic scattering amplitude[23].

The $R_{J_d L_d L_d'}(r)$ are the solution of radial equations corresponding to $J_d = L_d, L_d \pm 1$. The T_R tensor couples together the radial equations for $J_d = L_d + 1$ differing by two units of orbital angular momentum L_d' and similarly for $J_d = L_d - 1$.

If $X_{J_d L_d L'_d} = \rho R_{J_d L_d L'_d}$ where $\rho = k\,r$ the radial equations are

$$\frac{d^2 X_{J_d L_d L'_d}}{d\rho^2} + \left[1 + \alpha V_{J_d L'_d} - \frac{L'_d(L'_d+1)}{\rho^2}\right] X_{J_d L_d L'_d} = \beta\alpha V^t_{J_d}\, X_{J_d L_d L''}, \quad (1.13)$$

where $L'' = 2J_d - L'_d$

$$\beta = \delta_{J_d L_d+1} + \delta_{J_d L_d-1}$$

$$\alpha = E^{-1}_{\text{relative}} = \frac{2M_{dT}}{k^2 \hbar^2}$$

$$V_{JL} = -C + Vg(V) + i\left[W_v g(W) + Wf(W)\right]$$

$$-(S+iT)\,\frac{1}{r}\,\frac{dg(S)}{dr}\,K_{J_d L_d}(S) - Mf(R)K_{J_d L_d}(R) - Qf(L)K_{J_d L_d}(L)$$

$$V^t_{J_d} = Mf(R)K_{J_d}(R)$$

The $K_{J_d L_d}$ are eigenvalues for the corresponding operators and are given as follows:

J_d	$K_{J_d L_d}(S)$	$K_{J_d L_d}(R)$	$K_{J_d L_d}(L)$
L_d+1	L_d	$-\frac{L_d}{3(2L_d+3)}$	$\frac{1}{6}L_d(2L_d-1)$
L_d	-1	$\frac{1}{3}$	$-\frac{1}{6}(2L_d+3)(2L_d-1)$
L_d-1	$-L_d-1$	$-\frac{L_d+1}{3(2L_d-1)}$	$\frac{1}{6}(2L_d+3)(L_d+1)$

and $K_{J_d}(R) = \frac{\sqrt{J_d(J_d+1)}}{2J_d+1}$

Thus when $J_d = L_d$, $L'_d = L_d$ only, and a single uncoupled equation for $X_{L_d L_d L_d}$ is obtained. If $J_d = L_d + 1$ then $L'_d = L_d$, $L_d + 2$ and for $J_d = L_d - 1$, $L'_d = L_d$, $L_d - 2$. The coupled equations then involve either $X_{L_d+1 L_d L_d}$ and $X_{L_d+1 L_d L_d+2}$ or $X_{L_d-1 L_d L_d}$ and $X_{L_d-1 L_d L_d-2}$. The procedure for their solution has already been described[23]) (see also ref.[18])).

The equations are solved for the boundary conditions

$$R_{J_d L_d L'_d} \underset{r\to\infty}{=} (kr)^{-1} \left[e^{-2i\omega_{L'_d}} \Delta_{J_d L_d L'_d} A_{L'_d} + \delta_{L_d L'_d} B_{L_d} \right] e^{i\omega_{L'_d}} \qquad (1.14)$$

with

$$A_{L_d} = \frac{1}{2}(F_{L_d} - iG_{L_d}) \quad \text{and} \quad B_{L_d} = \frac{1}{2}(F_{L_d} + iG_{L_d})$$

where F_{L_d} and G_{L_d} are the standard Coulomb functions, and

$$\omega_{L_d} = \sum_{L=1}^{L_d} \tan^{-1}\left(\frac{\eta}{L}\right)$$

The coefficients $\Delta_{J_d L_d L'_d}$ may be obtained from the asymptotic relations (1.14); when the T_R tensor term in the deuteron-nucleus potential is set to zero they vanish in which case there is only one equation for each J_d value, with $L'_d = L_d$.

Expressions are now determined for the experimentally measurable quantities in terms of the transition matrix elements[24]) (see also ref.[17,25-27])).

Assuming that the incident deuteron beam and target nuclei are unpolarized the density matrix of the initial system is

$$\rho_i^I = \frac{\delta_{\mu_T\mu_T'}\,\delta_{\mu_d\mu_d'}}{3(2I_T+1)}$$

a square $3(2I_T+1)$ by $3(2I_T+1)$ matrix.

The final density matrix is then

$$\rho_f^I = R_I \rho_i^I R_I^\dagger$$

$$= \frac{1}{3(2I_T+1)} R_I R_I^\dagger$$

where $R_I R_I^\dagger$ has elements $R(\mu_d\mu_T \to \mu_p\mu_R)R^*(\mu_d\mu_T \to \mu_p'\mu_R')$ then

$$\rho^I_{\mu_p\mu_R\mu_p'\mu_R'} = \sum_{\mu_d\mu_T} \frac{1}{3(2I_T+1)} R(\mu_d\mu_T \to \mu_p\mu_R)R^*(\mu_d\mu_T \to \mu_p'\mu_R')$$

The matrix elements for the proton beam are obtained from this final density matrix by summing incoherently over μ_R i.e.

$$\rho^I_{\mu_p\mu_p'} = \sum_{\mu_R} \rho^I_{\mu_p\mu_R\mu_p'\mu_R}$$

so that the diagonal elements of $\rho^I_{\mu_p\mu_p'}$ are given by

$$\rho^I_{\mu_p\mu_p} = \frac{1}{3(2I_T+1)} \sum_{\mu_R\mu_d\mu_T} R(\mu_d\mu_T \to \mu_p\mu_R)\; R^*(\mu_d\mu_T \to \mu_p\mu_R)$$

The differential cross section is equal to

$$\frac{k_p M_{dT}}{k_d M_{pR}} \text{ trace } \rho^I$$

i.e.

$$\left(\frac{d\sigma}{d\Omega}\right)_{dp} = \frac{k_p M_{dT}}{k_d M_{pR}} \frac{1}{3(2I_T+1)} \sum_{\mu_d \mu_T \mu_p \mu_R} \left| R(\mu_d \mu_T \to \mu_p \mu_R) \right|^2 \qquad (1.15)$$

and the proton polarization is (choosing the y-axis perpendicular to the scattering plane)

$$\begin{aligned} P(\theta) &= \text{trace } (\sigma_y \rho^I)/\text{trace } \rho^I \\ &= i(\rho^I_{12} - \rho^I_{12})/(\rho^I_{11} + \rho^I_{22}) \\ &= i(\rho^{I*}_{21} - \rho^I_{21})/(\rho^I_{11} + \rho^I_{22}) \\ &= \frac{2\mathfrak{Im}\left[\sum_{\mu_R \mu_d \mu_T} R(\mu_d \mu_T \to -\tfrac{1}{2} \mu_R)\ R^*(\mu_d \mu_T \to \tfrac{1}{2} \mu_R)\right]}{\sum_{\mu_d \mu_T \mu_p \mu_R} |R(\mu_d \mu_T \to \mu_p \mu_R)|^2} \end{aligned} \qquad (1.16)$$

where for a spin half particle $\sigma_y = \begin{pmatrix} 0 & -i \\ i & 0 \end{pmatrix}$.

In the inverse reaction R(p,d)T an expression may be derived for the transition matrix elements $R(\mu_p \mu_R \to \mu_d \mu_T)$. For unpolarized protons incident on unaligned nuclei the density matrix of the initial system is

$$\rho_i^{II} = \frac{\delta_{\mu_R \mu'_R}\ \delta_{\mu_p \mu'_p}}{2(2I_R+1)}$$

and the final density matrix

$$\rho_f^{II} = R_{II}\, \rho_i^{II}\, R_{II}^{\dagger}$$

$$= \frac{1}{2(2I_R+1)}\, R_{II} R_{II}^{\dagger}$$

where $R_{II}R_{II}^{\dagger}$ has elements $R(\mu_p\mu_R \to \mu_d\mu_T)\ R^*(\mu_p\mu_R \to \mu_d'\mu_T')$ then

$$\rho^{II}_{\mu_d\mu_T\mu_d'\mu_T'} = \frac{1}{2(2I_R+1)} \sum_{\mu_p\mu_R} R(\mu_p\mu_R \to \mu_d\mu_T) R^*(\mu_p\mu_R \to \mu_d'\mu_T')$$

The matrix elements for the deuteron beam are obtained by summing incoherently over μ_T i.e.

$$\rho^{II}_{\mu_d\mu_d'} = \sum_{\mu_T} \rho^{II}_{\mu_d\mu_T\mu_d'\mu_T}$$

$$= \frac{1}{2(2I_R+1)} \sum_{\mu_p\mu_R\mu_T} R(\mu_p\mu_R \to \mu_d\mu_T)\ R^*(\mu_p\mu_R \to \mu_d'\mu_T)$$

The differential cross section for this reaction is

$$\frac{k_d M_{pR}}{k_p M_{dT}} \quad \text{trace} \quad \rho^{II}$$

i.e.

$$\left(\frac{d\sigma}{d\Omega}\right)_{pd} = \frac{k_d M_{pR}}{k_p M_{dT}} \frac{1}{2(2I_R+1)} \sum_{\mu_d\mu_p\mu_R\mu_T} |R(\mu_p\mu_R \to \mu_d\mu_T)|^2 \qquad (1.17)$$

Using a beam of polarized deuterons in a (d,p) reaction it is possible to determine the "analysing powers" of the deuteron beam by measuring the asymmetries of the scattered protons. These deuteron analysing powers for the (d,p) reaction with incident

polarized deuterons are identical to the corresponding deuteron polarizations (see eqn. (1.21)) in the inverse reaction initiated with unpolarized protons, for the same axes[28]). Similarly for the proton analysing power for a (p,d) reaction. In all the calculations presented in subsequent chapters the deuteron vector and tensor analysing powers for the (d,p) reaction are referred to a coordinate system with the z-axis anti-parallel to the incident deuteron momentum $\underline{k}_d$ and the y-axis along $\underline{k}_p \times \underline{k}_d$ where $\underline{k}_p$ is the outgoing proton momentum. Identical axes are used for the (p,d) reaction, the z-axis being parallel to the outgoing deuteron momentum $\underline{k}_d$ and the y-axis parallel to $\underline{k}_p \times \underline{k}_d$.

For this choice of axes, i.e.

for (p,d)	$\theta_{k_p} = \theta$	$\phi_{k_p} = \pi$
	$\theta_{k_d} = 0$	$\phi_{k_d} = 0$
and for (d,p)	$\theta_{k_p} = \pi - \theta$	$\phi_{k_p} = 0$
	$\theta_{k_d} = \pi$	$\phi_{k_d} = 0$

it may be shown that the transition matrix elements for the forward and inverse reaction are related

$$R(\mu_p \mu_R \rightarrow \mu_d \mu_T) = \frac{M_{dT}\theta_{j\ell}}{M_{pR}\theta^*_{j\ell}}(-1)^{\ell} R(\mu_d \mu_T \rightarrow \mu_p \mu_R)$$

hence

$$\left(\frac{d\sigma}{d\Omega}\right)_{pd} = \frac{k_d^2}{k_p^2} \frac{3(2I_T+1)}{2(2I_R+1)} \left(\frac{d\sigma}{d\Omega}\right)_{dp} \qquad (1.18)$$

The state of polarization of a beam of deuterons may be described in terms of the nine quantities $\langle T_{AB} \rangle$ [29],

$$T_{00} = 1$$

$$T_{10} = \sqrt{\frac{3}{2}}\ \sigma_z$$

$$T_{11} = -\frac{\sqrt{3}}{2}(\sigma_x + i\sigma_y)$$

$$T_{20} = \frac{1}{\sqrt{2}}\ (3\sigma_z^2 - 2)$$

$$T_{21} = -\frac{\sqrt{3}}{2}\ [(\sigma_x + i\sigma_y)\sigma_z + \sigma_z(\sigma_x + i\sigma_y)]$$

$$T_{22} = \frac{\sqrt{3}}{2}\ (\sigma_x + i\sigma_y) \qquad (1.19)$$

where for a spin one particle

$$\sigma_x = \frac{1}{\sqrt{2}} \begin{pmatrix} 0 & 1 & 0 \\ 1 & 0 & 1 \\ 0 & 1 & 0 \end{pmatrix}, \quad \sigma_y = \frac{1}{\sqrt{2}} \begin{pmatrix} 0 & -i & 0 \\ i & 0 & -i \\ 0 & i & 0 \end{pmatrix} \text{ and } \sigma_z = \begin{pmatrix} 1 & 0 & 0 \\ 0 & 0 & 0 \\ 0 & 0 & -1 \end{pmatrix}$$

also

$$T_{A-B} = (-1)^B\ T_{AB}^{\dagger}$$

and $$\langle T_{AB} \rangle = \text{trace}\ (\rho^{II}\ T_{AB})/\text{trace}\ \rho^{II}$$

where ρ^{II} is the density matrix for the deuteron beam. In terms of ρ^{II} the following relationships may be obtained (omitting the superscript II, remembering that ρ is the density matrix for the deuteron beam in a (p,d) reaction):

$$\langle T_{10} \rangle = \sqrt{\frac{3}{2}} (\rho_{11} - \rho_{33})/T$$

$$\langle T_{11} \rangle = -\sqrt{\frac{3}{2}} (\rho_{21} + \rho_{32})/T$$

$$\langle T_{20} \rangle = \frac{1}{\sqrt{2}} (\rho_{11} - 2\rho_{22} + \rho_{33})/T$$

$$\langle T_{21} \rangle = -\sqrt{\frac{3}{2}} (\rho_{21} - \rho_{32})/T$$

$$\langle T_{22} \rangle = \sqrt{3}\ \rho_{31}/T \qquad (1.20)$$

where $T = \rho_{11} + \rho_{22} + \rho_{33}$

It can be shown that for the axes chosen

$$R(-\mu_p - \mu_R \rightarrow -\mu_d - \mu_T) = (-1)^{\mu_d}(-1)^K R(\mu_p \mu_R \rightarrow \mu_d \mu_T)$$

where K is an integer. Using this result and noting that $\rho_{12} = \rho_{21}^*, \rho_{13} = \rho_{31}^*, \rho_{23} = \rho_{32}^*$ it can be shown that $\rho_{33} = \rho_{11}$, $\rho_{12} = -\rho_{23}^*$ and $\rho_{13} = \rho_{31}$. Thus for the above choice of axes the theoretical expressions for the experimentally measurable quantities become:

differential cross section

$$\left(\frac{d\sigma}{d\Omega}\right)_{pd} = \frac{k_d M_{pR}}{k_p M_{dT}} \frac{T}{2(2I_R+1)}$$

where $T = 2\rho_{11} + \rho_{22}$

vector polarizations

$$\langle T_{10} \rangle = 0$$

$$\langle T_{11} \rangle = -\sqrt{\frac{3}{2}} (\rho_{21} - \rho_{21}^*)/T$$

tensor polarizations

$$\langle T_{20} \rangle = \sqrt{2}\ (\rho_{11} - \rho_{22})/T$$

$$\langle T_{21} \rangle = -\sqrt{\frac{3}{2}}\ (\rho_{21} + \rho_{21}^{*})/T$$

$$\langle T_{22} \rangle = \sqrt{3}\ \rho_{31}/T \qquad (1.21)$$

1.3 Finite-range formulation including the D-state of the deuteron

In general the interaction V_{np} for the deuteron, as well as the usual central term, may contain a spin-orbit interaction and a non-central term, it is the non-central term which gives rise to the small D-state component in the internal deuteron wave function. The angular part of the D-state component corresponding to $\phi_d(\underline{r}_d)$ of eqn.(1.3) is coupled to the deuteron spin wave function. Consequently when the D-state component is included in the deuteron bound-state wave function, the expansion analogous to eqn.(1.3) is

$$\Psi(\underline{r}_d,\underline{r}_{dT},\mu_d) = \sum_{J_d L_d L_d' M_d} 4\pi i^{L_d} Y_{L_d}^{M_d}(\Omega_{k_d})^{*}\, C(L_d 1 J_d, M_d \mu_d M_d+\mu_d)$$

$$\cdot\ R_{J_d L_d L_d'}(r_{dT}) \sum_{\ell_d \mu_d'} v_{\ell_d}(r_d)\, \mathcal{Y}_{1\ell_d 1}^{\mu_d'}$$

$$\cdot\ C(L_d' 1 J_d, M_d+\mu_d-\mu_d'\mu_d' M_d+\mu_d)\ Y_{L_d'}^{M_d+\mu_d-\mu_d'}(\Omega_{dT}) \qquad (1.22)$$

where $\mathcal{Y}_{1\ell_d 1}^{\mu_d'} = \sum_{m_d} C(1\ell_d 1, \mu_d'-m_d m_d \mu_d')\, Y_{\ell_d}^{m_d}(\Omega_d)\, \chi_1^{\mu_d'-m_d}$

The radial parts of the internal deuteron wave function for orbital angular momenta $\ell_d = 0$ and 2 (component m_d) are given by $v_{\ell_d}(r_d)$, and $\mathcal{Y}^{\mu'_d}_{1\ell_d 1}$ denote the spin-angle parts. Eqn.(1.2) and eqn.(1.22) may then be substituted into eqn.(1.5). The potential $V_{np}(\underline{r}_d)$ was taken to be the soft-core interaction of Reid[14])

$$V_{np} = V_c + V_T\, S_{pn} + V_{LS}\, \underline{L} \cdot \underline{S}$$

where

$$V_c = -h\, e^{-x}/x + 105.468\, e^{-2x}/x - 3187.8\, e^{-4x}/x + 9924.3\, e^{-6x}/x \quad ,$$

$$V_T = -h\left[(1 + 3/x + 3/x^2)e^{-x} - (12/x + 3/x^2)e^{-4x}\right]/x + 351.77\, e^{-4x}/x - 1673.5\, e^{-6x}/x,$$

$$V_{LS} = 708.91\, e^{-4x}/x - 2713.1\, e^{-6x}/x,$$

$$h = 10.463 \text{ MeV} \quad , \qquad x = 0.7\, r_d$$

and $S_{pn} = 3(\underline{\sigma}_p \cdot \underline{r}_d)(\underline{\sigma}_n \cdot \underline{r}_d)r_d^{-2} - (\underline{\sigma}_p \cdot \underline{\sigma}_n)$ is the usual tensor operator. Thus

$$V_{np}\left[v_0 \mathcal{Y}^{\mu'_d}_{101} + v_2 \mathcal{Y}^{\mu'_d}_{121}\right] = u_0 \mathcal{Y}^{\mu'_d}_{101} + u_2 \mathcal{Y}^{\mu'_d}_{121} \tag{1.23}$$

where

$$u_0 = V_c\, v_0 + \sqrt{8}\, V_T\, v_2$$

and

$$u_2 = (V_c - 2V_T - 3V_{LS})v_2 + \sqrt{8}\, V_T\, v_0$$

Noting that

$$\chi_1^{\mu'_d - m_d} = \sum_{\mu_p} C(\tfrac{1}{2}\,\tfrac{1}{2}\,1, \mu_n \bar{\mu}_p \mu'_d - m_d)\, \chi_{\frac{1}{2}}^{\mu_n}\, \chi_{\frac{1}{2}}^{\bar{\mu}_p} \quad ,$$

and

$$\chi^{\mu'_p\dagger}_{\frac{1}{2}} \chi^{\bar{\mu}_p}_{\frac{1}{2}} = \delta_{\mu'_p\bar{\mu}_p} ,$$

$$\chi^{\mu_j-m\dagger}_{\frac{1}{2}} \chi^{\mu'_d-m_d-\mu'_p}_{\frac{1}{2}} = \delta_{\mu_j-m\ \mu'_d-m_d-\mu'_p} ,$$

i.e.
$$m_d = m - \mu_j + \mu'_d - \mu'_p \tag{1.24}$$

the elements of the transition matrix may be obtained:

$$R(\mu_d\mu_T\to\mu_p\mu_R) = -\frac{M_{pR}}{2\pi\hbar^2} \sum_{\substack{J_dJ_pL_dL'_dL_p \\ j\ell M_dM_p}} (4\pi)^2 i^{L_d-L_p-\ell}\, \theta^*_{j\ell L_p}(\Omega_{k_p})\, Y^{M_p}_{L_p}(\Omega_{k_p})\, Y^{M_d}_{L_d}(\Omega_{k_d})^*$$

$$\cdot\, C(I_TjI_R,\mu_T\mu_j\mu_R)C(L_p\tfrac{1}{2}J_p,M_p\mu_pM_p+\mu_p)C(L_dlJ_d,M_d\mu_dM_d+\mu_d)$$

$$\cdot \sum_{\mu'_d\mu'_p\ell_dm} C(\ell\tfrac{1}{2}j,m\ \mu_j-m\ \mu_j)C(l\ell_dl,\mu_j+\mu'_p-m\ m-\mu_j+\mu'_d-\mu'_p\mu'_d)$$

$$\cdot\, C(L_p\tfrac{1}{2}J_p,M_p+\mu_p-\mu'_p\mu'_pM_p+\mu_p)C(L'_dlJ_d,M_d+\mu_d-\mu'_d\mu'_dM_d+\mu_d)$$

$$\cdot\, C(\tfrac{1}{2}\tfrac{1}{2}l,\mu_j-m\ \mu'_p\ \mu_j+\mu'_p-m)\mathcal{J} \tag{1.25}$$

where

$$\mathcal{J} = \int R_{J_pL_p}(r_{pR})R_{J_dL_dL'_d}(r_{dT})u_{j\ell}(r_{nT})u_{\ell_d}(r_d)$$

$$\cdot\, Y^{M_p+\mu_p-\mu'_p}_{L_p}(\Omega_{pR})^*\, Y^{M_d+\mu_d-\mu'_d}_{L'_d}(\Omega_{dT})\, Y^{m}_{\ell}(\Omega_{nT})^*\, Y^{m-\mu_j+\mu'_d-\mu'_p}_{\ell_d}(\Omega_d)$$

$$\cdot\, d\underline{r}_{nT}\, d\underline{r}_{pR}$$

To avoid expanding the deuteron and proton distorted waves

the coordinates of integration are transformed from $\underline{r}_{nT}$ and $\underline{r}_{pR}$ to $\underline{r}_{dT}$ and $\underline{r}_{pR}$, introducing a Jacobian J. The coordinates $\underline{r}_{nT}$ and $\underline{r}_{d}$ may be written as a linear combination of the new coordinates of integration (see Appendix):

$$\underline{r}_{nT} = s_1\underline{r}_{pR} + t_1\underline{r}_{dT}$$

$$\underline{r}_{d} = s_2\underline{r}_{pR} + t_2\underline{r}_{dT}$$

and $J = (t_1)^3$ (as before).

Using the procedure of Austern et al[30]) the following expansions may be performed[31])

$$r_{nT}^{\ell}\, Y_{\ell}^{m}(\Omega_{nT})^{*} = \sum_{\lambda=0}^{\ell}\sum_{\mu}\left[\frac{4\pi(2\ell+1)(2\ell)!}{(2\lambda+1)(2\ell-2\lambda+1)(2\lambda)!(2\ell-2\lambda)!}\right]^{1/2}(s_1 r_{pR})^{\ell-\lambda}(t_1 r_{dT})^{\lambda}$$

$$C(\ell-\lambda\lambda\ell, m-\mu\mu m)\, Y_{\ell-\lambda}^{m-\mu}(\Omega_{pR})^{*}\, Y_{\lambda}^{\mu}(\Omega_{dT})^{*} \qquad (1.26)$$

and

$$r_d^{\ell_d}\, Y_{\ell_d}^{m_d}(\Omega_d) = \sum_{\lambda'=0}^{\ell_d}\sum_{\mu'}\left[\frac{4\pi(2\ell_d+1)(2\ell_d)!}{(2\lambda'+1)(2\ell_d-2\lambda'+1)(2\lambda')!(2\ell_d-2\lambda')!}\right]^{1/2}(t_2 r_{dT})^{\ell_d-\lambda'}$$

$$(s_2 r_{pR})^{\lambda'}\, C(\ell-\lambda'\lambda'\ell_d, m_d-\mu'\mu' m_d)\, Y_{\ell_d-\lambda'}^{m_d-\mu'}(\Omega_{dT})\, Y_{\lambda'}^{\mu'}(\Omega_{pR}) \qquad (1.27)$$

where from eqn.(1.24) $m_d = m - \mu_j + \mu_d' - \mu_p'$.

Also, after applying the addition theorem for Legendre polynomials[19]):

$$\frac{u_{\ell_d}(r_d)u_{j\ell}(r_{nT})}{r_d^{\ell_d} r_{nT}^{\ell}} = 2\pi \sum_{K=0}^{\infty} \sum_{Q} g_{K\ell_d j\ell}(r_{dT}, r_{pR})\, Y_K^Q(\Omega_{dT})^*\, Y_K^Q(\Omega_{pR}) \quad (1.28)$$

where on inversion[32])

$$g_{K\ell_d j\ell}(r_{dT}, r_{pR}) = \int_{-1}^{+1} \left[\frac{u_{\ell_d}(r_d)u_{j\ell}(r_{nT})}{r_d^{\ell_d} r_{nT}^{\ell}}\right] P_K(\omega)\, d\omega \quad (1.29)$$

$P_K(\omega)$ is the usual Legendre polynomial and ω is the cosine of the angle between $\underline{r}_{dT}$ and $\underline{r}_{pR}$.

If the spherical harmonic addition theorem is applied[19])

$$Y_K^Q(\Omega_{pR}) Y_{\lambda'}^{\mu'}(\Omega_{pR}) = \sum_{\Lambda} \left[\frac{(2K+1)(2\lambda'+1)}{4\pi(2\Lambda+1)}\right]^{1/2} C(K\lambda'\Lambda, Q\mu' Q+\mu') C(K\lambda'\Lambda, 000)$$

$$\cdot\, Y_{\Lambda}^{Q+\mu'}(\Omega_{pR})$$

and

$$Y_{\lambda}^{\mu}(\Omega_{dT})^*\, Y_K^Q(\Omega_{dT})^* = \sum_{\Lambda'} \left[\frac{(2\lambda+1)(2K+1)}{4\pi(2\Lambda'+1)}\right]^{1/2} C(\lambda K\Lambda', \mu Q Q+\mu) C(\lambda K\Lambda' 000)\, Y_{\Lambda'}^{Q+\mu}(\Omega_{dT})^*$$

then for each of the angular coordinates Ω_{pR} and Ω_{dT}, an integral over three spherical harmonics results. Performing these integrals gives the relations

$$Q = M_p + \mu_p + \mu_j - \mu_d' - \mu + m_d - \mu'$$

and $$M_d = M_p + \mu_p + \mu_j - \mu_d\,, \quad (1.30)$$

as in eqn.(1.8).

Consequently the integrals in eqn.(1.25) become

$$\mathcal{J} = \frac{1}{2} \sum_{K\lambda\lambda'\Lambda\Lambda'} \frac{(2K+1)}{(2\Lambda+1)(2\Lambda'+1)} \left[(2L_p+1)(2L'_d+1)(2\ell+1)(2\ell_d+1)\right]^{1/2} \begin{pmatrix} 2\ell \\ 2\lambda \end{pmatrix}^{1/2} \begin{pmatrix} 2\ell_d \\ 2\lambda' \end{pmatrix}^{1/2}$$

$$\cdot\ C(K\lambda'\Lambda,000)C(\ell-\lambda L_p\Lambda,000)C(L'_d\ell_d-\lambda\Lambda',000)C(\lambda K\Lambda',000)$$

$$\cdot\ \sum_{\mu\mu'} C(\ell-\lambda\lambda\ell,m-\mu\mu m)C(\ell-\lambda L_p\Lambda,m-\mu M_p+\mu_p-\mu'_p M_p+\mu_p-\mu'_p+m-\mu)$$

$$\cdot\ C(\ell_d-\lambda'\lambda'\ell_d,m-\mu_j+\mu'_d-\mu'_p-\mu'\mu'\ m-\mu_j+\mu'_d-\mu'_p)$$

$$\cdot\ C(K\lambda'\Lambda,M_p+\mu_p-\mu+m-\mu'_p-\mu'\mu'\ M_p+\mu_p-\mu+m-\mu'_p)$$

$$\cdot\ C(\lambda K\Lambda',\mu M_p+\mu_p-\mu+m-\mu'_p-\mu' M_p+\mu_p+m-\mu'_p-\mu')$$

$$\cdot\ C(L'_d\ell_d-\lambda'\Lambda',M_d+\mu_d-\mu'_d m-\mu_j+\mu'_d-\mu'_p-\mu' M_p+\mu_p+m-\mu'_p-\mu')$$

$$\cdot\ I_{J_pL_pJ_dL_dL'_dK\ell j\lambda\lambda'\ell_d} \qquad (1.31)$$

where

$$I_{J_pL_pJ_dL_dL'_dK\ell j\lambda\lambda'\ell_d} = J \int R_{J_pL_p}(r_{pR}) R_{J_dL_dL'_d}(r_{dT}) g_{K\ell_d j\ell}(r_{dT},r_{pR})$$

$$\cdot\ (s_1 r_{pR})^{\ell-\lambda} (t_1 r_{dT})^{\lambda} (t_2 r_{dT})^{\ell_d-\lambda'} (s_2 r_{pR})^{\lambda'}$$

$$r^2_{pR} r^2_{dT} dr_{pR} dr_{dT}$$

and $\begin{pmatrix} x \\ y \end{pmatrix} = \dfrac{x!}{y!(x-y)!}$

The summations over μ', μ, μ'_p may each be performed using the general relation[25])

$$\sum_{\gamma} C(acf,\alpha\gamma\alpha+\gamma)C(bdf',\varepsilon-\alpha\omega-\varepsilon-\gamma\omega-\gamma-\alpha)$$

$$\cdot\, C(ff'g,\alpha+\gamma\omega-\alpha-\gamma\omega)C(cde',\gamma\omega-\varepsilon-\gamma\omega-\varepsilon)$$

$$= \sum_{e} \left[(2e+1)(2e'+1)(2f+1)(2f'+1)\right]^{1/2} X(abe,cde',ff'g)$$

$$\cdot\, C(ee'g,\varepsilon\omega-\varepsilon\omega)C(abe,\alpha\varepsilon-\alpha\varepsilon)$$

and those over m, μ_d' using

$$\sum_{\beta} C(abe,\alpha\beta\alpha+\beta)C(edc,\alpha+\beta\delta\alpha+\beta+\delta)C(bdf,\beta\delta\beta+\delta)$$

$$= \left[(2e+1)(2f+1)\right]^{1/2} W(abcd,ef)C(afc,\alpha\beta+\delta\alpha+\beta+\delta)$$

where the X and W coefficients are as defined in ref.[22]). This gives for the transition matrix elements

$$R(\mu_d\mu_T\rightarrow\mu_p\mu_R) = \frac{-8\pi M_{pR}}{\hbar^2} \sum_{\substack{\ell_j \ell_d J_p L_p M_p \\ J_d L_d L_d'}} i^{L_d-L_p-\ell}\, \theta^*_{j\ell}$$

$$\cdot\, Y^{M_p}_{L_p}(\Omega_{k_p}) Y^{M_p+\mu_p+\mu_j-\mu_d}_{L_d}(\Omega_{k_d})^* C(I_T j I_R, \mu_T \mu_j \mu_R)$$

$$\cdot\, C(L_p\, 1/2\, J_p, M_p \mu_p M_p+\mu_p) C(L_d\, l\, J_d, M_p+\mu_p+\mu_j-\mu_d \mu_d M_p+\mu_p+\mu_j) Q \qquad (1.32)$$

where

$$Q = \frac{3}{2} \sum_{\substack{K\lambda\lambda'\Lambda\Lambda' \\ eyv}} I_{J_p L_p J_d L_d L'_d K \ell j \lambda\lambda' \ell_d} (-1)^{M_p+\mu_p-J_d+\ell+y-v}$$

$$\cdot (2K+1)(2\ell+1)(2\ell_d+1)(2e+1)(2y+1)(2v+1)\left[(2L'_d+1)(2J_p+1)(2J_d+1)(2L_p+1)\right]^{1/2}$$

$$\cdot \begin{pmatrix} 2\ell \\ 2\lambda \end{pmatrix}^{1/2} \begin{pmatrix} 2\ell_d \\ 2\lambda' \end{pmatrix}^{1/2} C(K\lambda'\Lambda,000)C(\ell-\lambda L_p \Lambda,000)C(L'_d \ell_d-\lambda'\Lambda',000)C(\lambda K\Lambda',000)$$

$$\cdot W(L'_d \ell v\tfrac{1}{2},yj)W(J_p 1jL'_d,vJ_d)$$

$$\cdot C(J_p J_d j,-M_p-\mu_p\ M_p+\mu_p+\mu_j\mu_j)X(\Lambda L'_d e,\lambda'\ell_d-\lambda'\ell_d,K\Lambda'\Lambda)$$

$$\cdot X(\ell L'_d y,\lambda e\ell_d,\ell-\lambda\Lambda L_p)X(J_p 1v,\tfrac{1}{2}1\tfrac{1}{2},L_p\ell_d y)$$

Performing the summation over e:

$$\sum_e (2e+1)\ X(\Lambda L'_d e,\lambda'\ell_d-\lambda'\ell_d,K\Lambda'\lambda)$$

$$\cdot X(\ell L'_d y,\lambda e\ell_d,\ell-\lambda\Lambda L_p)$$

$$= \sum_u (2u+1)\ W(\ell\lambda L_p\Lambda,\ell-\lambda u)\ W(\ell L'_d L_p \ell_d,yu)$$

$$\cdot W(\Lambda'\lambda\lambda'\Lambda,Ku)\ W(\Lambda' L'_d\lambda'\ell_d,\ell_d-\lambda' u)$$

allows the summations over y and v to be carried out:

$$\sum_{y,v} (-1)^{y-v} (2y+1)(2v+1)W(L'_d\ell v\tfrac{1}{2},yj)W(J_p 1jL'_d,vJ_d)$$

$$\cdot W(\ell L'_d L_p \ell_d,yu)X(J_p 1v,\tfrac{1}{2}1\tfrac{1}{2},L_p\ell_d y)$$

$$= (-1)^{\ell-j} W(1J_d\ell_d L'_d,u1)X(\tfrac{1}{2}J_p L_p,\tfrac{1}{2}j\ell,1J_d u)$$

Thus Q in eqn.(1.32) reduces to

$$Q = \frac{3}{2} \sum_{K\lambda\lambda'\Lambda\Lambda' u} I_{J_p L_p J_d L_d L'_d K \ell j \lambda\lambda' \ell_d} (-1)^{M_p+\mu_p-J_d-j}$$

$$\cdot\ (2u+1)(2K+1)(2\ell+1)(2\ell_d+1)\left[(2L'_d+1)(2J_p+1)(2J_d+1)(2L_p+1)\right]^{1/2}$$

$$\cdot \begin{pmatrix} 2\ell \\ 2\lambda \end{pmatrix}^{1/2} \begin{pmatrix} 2\ell_d \\ 2\lambda' \end{pmatrix}^{1/2} C(K\lambda'\Lambda,000)\,C(\ell-\lambda L_p \Lambda,000)\,C(L'_d \ell_d \lambda'\Lambda',000)\,C(\lambda K\Lambda',000)$$

$$\cdot\ C(J_p J_d j,-M_p-\mu_p\ M_p+\mu_p+\mu_j\ \mu_j)\,X(\tfrac{1}{2}J_p L_p,\tfrac{1}{2}j\ell,1J_d u)$$

$$\cdot\ W(\ell\lambda L_p\Lambda,\ell-\lambda u)\,W(\Lambda'\lambda\lambda'\Lambda,Ku)\,W(\Lambda' L'_d \lambda' \ell_d,\ell_d-\lambda' u)$$

$$\cdot\ W(1J_d \ell_d L'_d,ul)$$

The coefficients $g_{K\ell_d j\ell}$ may be evaluated when the $u_{\ell_d}(r_d)$ are obtained by interpolation of the tabulated wave functions $r_d v_{\ell_d}(r_d)$ of ref.[14]) and multiplication by the appropriate potentials as required by eqn.(1.23).

In the evaluation of the radial integrals $I_{J_p L_p J_d L_d L'_d K \ell j \lambda\lambda' \ell_d}$ the variable r_{dT} was incremented in small steps and at each step r_{pR} was given values in the range $r_{dT} \pm 0.9$ fm with increments of 0.1 fm. The coefficients $g_{K\ell_d j\ell}(r_{dT}, r_{pR})$ were computed at each of the points in this grid.

The scalar relationships corresponding to eqns.(A.5) and (A.6) of the Appendix are

$$r_{nT} = \left[\frac{m_d\, M_R}{m_n (M_T+m_d)}\right]\left[r_{dT}^2 + \left(\frac{m_p}{m_d}\right)^2 r_{pR}^2 - 2\left(\frac{m_p}{m_d}\right) r_{dT}\, r_{pR}\, \omega\right]^{1/2}$$

$$r_d = \left[\frac{m_d\, M_R}{m_n (M_T+m_d)}\right]\left[\left(\frac{M_T}{M_R}\right)^2 r_{dT}^2 + r_{pR}^2 - 2\left(\frac{M_T}{M_R}\right) r_{dT}\, r_{pR}\, \omega\right]^{1/2} \qquad (1.33)$$

Thus the integral of eqn.(1.29) may be performed, since for given values of r_{dT} and r_{pR} the integrand is a function of ω the cosine of the angle between $\underline{r}_{dT}$ and $\underline{r}_{pR}$. At each increment of ω, $u_{\ell_d}(r_d)$ and $u_{j\ell}(r_{nT})$ were read from the respective tables of the functions, after r_d and r_{nT} had been evaluated using the relations (1.33). These functions were truncated at $r_d \sim 13$ fm and $r_{nT} \sim 24$ fm respectively. A preliminary numerical analysis indicated that in general for increasing r_{dT} the integrands of eqn.(1.29) tended to a maximum magnitude at $\omega \sim 1$ and diminished rapidly for values less than 1, so that a variable step length was necessary for the integration over ω.

The maximum value of K was restricted by the maximum L value used in the deuteron and proton channels. Generally, the selection rules determining which terms contribute to the summations of eqn.(1.32) may be obtained from the various triads implicit in the Racah algebra.

CHAPTER 2

j-DEPENDENCE IN ^{50,52}Cr(d,p) REACTIONS

2.1 Introduction

There is considerable experimental evidence that the angular distribution of the (d,p) reaction depends not only upon the orbital angular momentum ℓ but also upon the total angular momentum j of the captured neutron. The effect is very marked for bombarding energies of 7 to 12 MeV in the case of $\ell = 1$ transitions from spin-zero target nuclei of atomic number $40 \lesssim A \lesssim 70$ to $J = \frac{1}{2}$ and $J = \frac{3}{2}$ final states[4,33-50]. In general, the distributions involving $J = \frac{1}{2}$ residual states show a characteristic minimum at backward angles which is absent or much less pronounced in the distributions leading to $J = \frac{3}{2}$ levels. Previous attempts[42,46,48,51,52] to describe these results using the DW theory including spin-orbit interactions in both the deuteron and proton OM potentials have met with mixed success varying from no agreement to qualitative agreement with experiment.

It is of interest to investigate further whether the discrepancies between the DW predictions and experiment are due to inadequacies in the theory, approximations in the calculations or simply arise from using the wrong parameters. In connection with the second possibility, it has been shown[10,53] that including the D-state of the deuteron[54,55], (see chapter 1 where an exact FR D-state formulation is discussed) or possible deuteron-nucleus

tensor interactions in the DW calculations (see chapter 3) has only a relatively small effect on the j-dependence of $\ell = 1$ transitions. Calculations [6]) including non-local and FR corrections suggest that the shapes of the angular distributions are very similar to those obtained using the corresponding local, ZR potential, therefore the use of the simpler potential is not likely to seriously affect the j-dependence of the cross sections. The assumptions of single particle form factors for $2p_{1/2}$ or $2p_{3/2}$ captured neutrons obtained using the "well-depth" prescription is expected[56]) to be satisfactory for targets of neutron number $N \lesssim 28$ (as studied in the present work) corresponding to a closed $f_{7/2}$ shell in the strict single-particle model (however see also ref.[57])). In other cases in which configuration mixing is important, no detailed study has been carried out to investigate the effect on the j-dependence of the angular distributions, although there is some evidence that the empirical rule persists in such cases[49]).

Irrespective of the agreement between theory and experiment, an empirical rule is very useful for assigning spins to levels in residual nuclei. However, the reaction $^{50}Cr(d,p)^{51}Cr$(1.895 MeV state) appears to be a definite exception to the rule since near 8 MeV (ref.[33,43])), the angular distribution has a large dip near 125° while the γ-γ correlation work[58]) gives unambiguously $J = 3/2$ for this level. Such exceptions make the value of the rule rather dubious.

In this chapter, several $\ell = 1$ transitions in the reaction $^{52}Cr(d,p)^{53}Cr$ and $^{50}Cr(d,p)^{51}Cr$ are studied to test the adequacy

of the DW theory, and in particular the anomalous transition to the 1.895 MeV level in ^{51}Cr is investigated.

2.2 The ^{52}Cr(d,p)^{53}Cr reaction

2.2.1 DW Analysis

Several studies of the reaction ^{52}Cr(d,p)^{53}Cr have been reported[33-35]) for deuteron bombarding energies in the range 7 to 11 MeV, and four strong ℓ = 1 transitions leading to the ground state (g.s.) and the 0.57, 2.32 and 3.61 MeV excited states in ^{53}Cr are observed. Deuteron vector analysing power measurements[36-39]) unambiguously assign spins to these states of $\frac{3}{2}$, $\frac{1}{2}$, $\frac{3}{2}$ and $\frac{1}{2}$ respectively and these values are assumed in the present work.

DW calculations were performed using the OM potential described in chapter 1 for 8 MeV incident deuteron energy. The OM parameters which were varied to give the best overall fit to the four cross sections shown in fig. 2.1 are given in table 2.1. The proton parameters were taken close to conventional values.

It was found that the deuteron parameters of table 2.1 do not fit the elastic scattering data[40]) very well, and any attempt to improve this description tended to destroy the agreement for the reaction cross sections. While the whole of parameter space could not be searched, it seems probable that rather different deuteron parameters (differing by 10–20%) are required to describe the elastic scattering and reaction data. This implies that

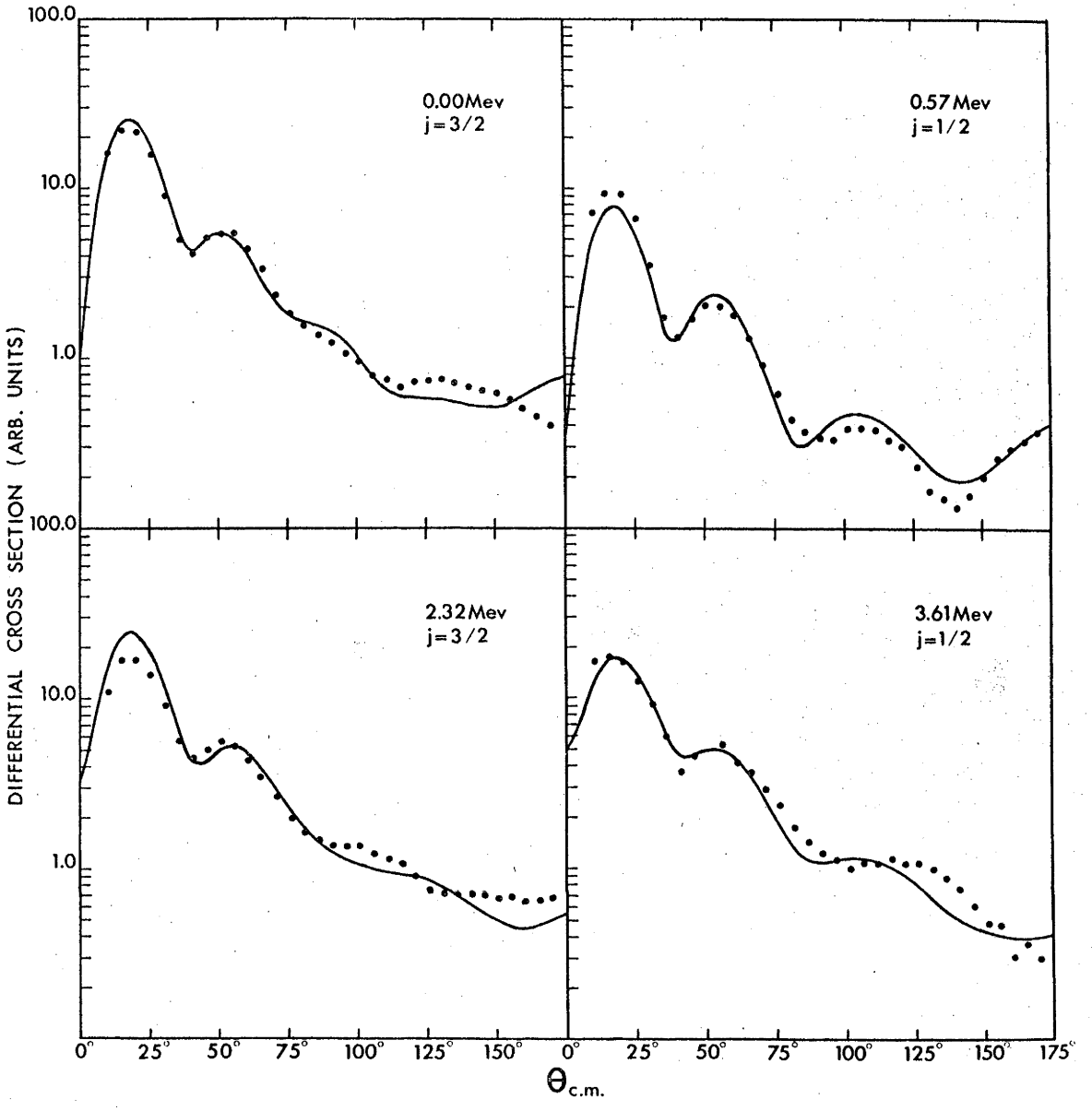

Fig. 2.1. Differential cross sections for the reaction $^{52}Cr(d,p)^{53}Cr$ leading to the ground, 0.57, 2.32 and 3.61 MeV states in ^{53}Cr at 8 MeV bombarding energy. The solid curves are distorted wave calculations for the parameters of Table 2.1 and the points are the data of ref.[33]).

Table 2.1

POTENTIALS

	Deuteron	Proton	Neutron
V (MeV)(a) ^{52}Cr	100	53	adjusted
(b) ^{50}Cr	108[c])	55	adjusted
r_v(fm)	1.175	1.250	1.250
a_v(fm)	0.782	0.650	0.650
W (MeV)	18	10	
r_w(fm)	1.455	1.250	
a_w(fm)	0.600	0.470	
S (MeV fm^2)	18	16	
T (MeV fm^2)	-10	0	
r_s(fm)	0.700	1.250	
a_s(fm)	0.400	0.650	
r_c(fm)	1.300	1.250	

[c]) A value of 120 MeV was used in the $j = \frac{3}{2}$ calculation for the transition to the 1.895 MeV level.

either the optical model or the DW theory (or both) is not strictly valid, and that the different potentials are required to partially compensate for deficiencies in these models, for example the lack of a correct treatment of the distortion and break-up of the deuteron[59]). The parameters, which best describe the asymptotic behaviour of the deuteron wave function and hence the elastic scattering results, are not necessarily the same as those which optimize the deuteron wave function in the vicinity of the nuclear surface where the contribution to the reaction cross section is largest. Fig. 2.1 shows that the essential features of the j-dependence are qualitatively described in terms of the DW theory for parameters which are different but fairly close to those required to describe the corresponding elastic scattering data. The neutron spin-orbit potential was found to have a small effect on the shapes of the cross sections so that the j-dependent effect arises primarily as a consequence of the spin-orbit terms in the deuteron and proton potentials (this is true also of the proton polarization and deuteron vector analysing power ref.[60])). The fit to any single reaction cross section could be improved by allowing the parameters to vary slightly from level to level; in principle this is not unreasonable, since the "corrections" may be different in each case. If the corrections for each level tend to produce a similar modification of the OM parameters, then a rule such as the Lee-Schiffer criterion[41,46]) is possible. However, if in occasional cases quite large variations in the parameters occur, the general rule can be expected to fail. Fig. 2.2 shows the corresponding predictions for the deuteron vector

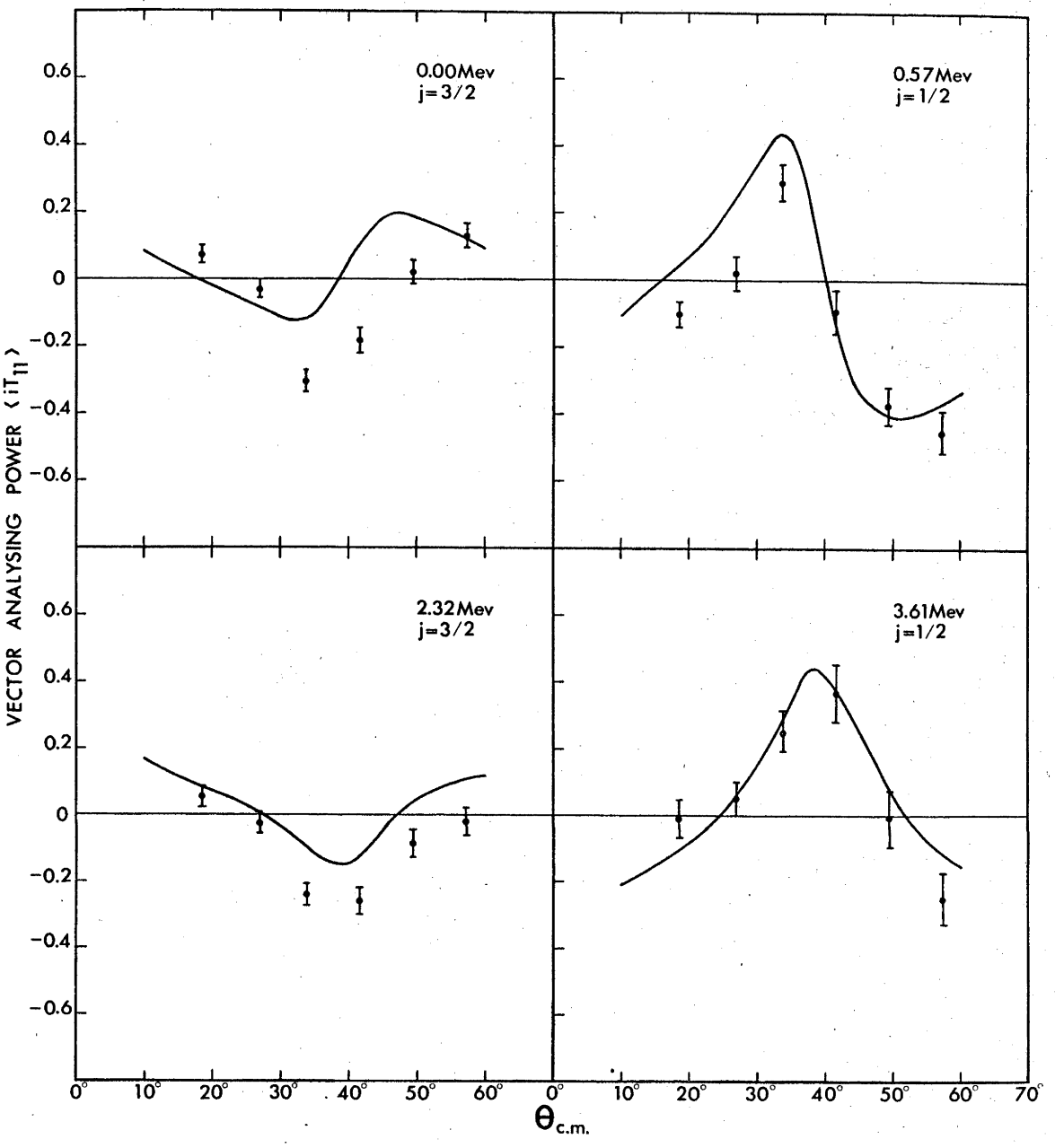

Fig. 2.2. Deuteron vector analysing powers for the reaction $^{52}Cr(d,p)^{53}Cr$ leading to the ground, 0.57, 2.32 and 3.61 MeV states in ^{53}Cr at 8 MeV bombarding energy. The solid curves are distorted wave calculations for the parameters of Table 2.1 and the points are the data of ref.[36]).

Table 2.2

SPECTROSCOPIC FACTORS FOR THE $^{52}Cr(d,p)^{53}Cr$ REACTION

Level E_x(MeV)	Q (MeV)	(2J+1)S	$J^{d)}$	S $J = \frac{1}{2}$	S $J = \frac{3}{2}$
0.00	5.73	2.88[a)]	$\frac{3}{2}$	-	0.72
0.57	5.16	0.78[a)]	$\frac{1}{2}$	0.39	-
2.32	3.41	1.59[a)]	$\frac{3}{2}$	-	0.40
2.68	3.05	0.12[b)]	$(\frac{3}{2})$	-	0.03
2.72	3.01	0.05[b)]	$\frac{1}{2}$	0.03	-
3.19	2.54	0.05[b)]	$(\frac{3}{2})$	-	0.01
3.61	2.12	0.91[a)]	$\frac{1}{2}$	0.45	-
4.05	1.68	0.01[b)]	$(\frac{1}{2})$	0.01	-
4.07	1.66	0.03[b)]	$(\frac{3}{2})$	-	0.01
4.61	1.12	0.20[b)]	$(\frac{1}{2})$	0.10	-
5.39	0.34	0.12[c)]	$(\frac{1}{2})$	0.06	-
5.45	0.28	0.07[c)]	$(\frac{3}{2})$	-	0.02
5.55	0.18	0.02[c]	$(\frac{1}{2})$	0.01	-
	Sum	6.83		1.05	1.19

[a)]present work [b)]ref.[34]) [c)]ref.[35]) [d)]Tentative spin assignments are indicated in parentheses. Preferred values are partially arbitrary and partially based upon $2p_{1/2}$ and $2p_{3/2}$ sum rules and shell model systematics.

analysing powers[36,37]) for the four transitions. Although these results were not included in the fitting procedure, it is seen that the curves give a satisfactory description of the data.

2.2.2 Spectroscopic Factors

Relative spectroscopic factors S/S_o, where S_o is the spectroscopic factor for the g.s., were obtained for the four strong transitions by normalizing the DW predictions to the relative experimental data to give an overall best fit. In each case the cross section was calculated in the usual ZR approximation[17]) and was multiplied by a FR correction factor of 1.65. The value of S_o was found by performing the g.s. calculation at 7.5 MeV bombarding energy for the same OM parameters and comparing with the absolute cross-section measurements of Rao et al[34]). In this manner, spectroscopic factors S were obtained for these strong transitions.

If the spin J of the residual nucleus is unknown, only the spectroscopic transition strength $(2J + 1)S$ can be determined from the DW analysis. Table 2.2 gives the values of $(2J + 1)S$ for the $\ell = 1$ transitions where the strengths for the weaker transitions were taken from previous analyses[34,35]). The sum of the strengths $(2J + 1)S$ is 6.8 which is in good agreement with the expected value of 6.0 for the extreme single-particle model considering the uncertainties in the experimental cross sections and in the DW calculations. In this simple picture, the separate sums for the $2p_{1/2}$ and $2p_{3/2}$ transitions are 2.0 and 4.0,

respectively, and corresponding in both cases to a spectroscopic factor of unity spread over several states. The spins of some of the states have been established, namely g.s. as $\frac{3}{2}$ ref.[61]), 0.57 MeV as $\frac{1}{2}$ ref.[62,63]), 2.32 MeV as $\frac{3}{2}$ ref.[62,63]), 2.72 MeV as $\frac{1}{2}$ ref.[63]) and 3.61 MeV as $\frac{1}{2}$ ref. [36,37]). The spins of the remaining states are given in table 2.2 (in parentheses) where the values chosen are partially arbitrary and partially based upon the $2p_{1/2}$ and $2p_{3/2}$ sum rules and shell-model systematics. For example, the 4.61 and 5.39 MeV states were taken to have spin $\frac{1}{2}$ because of their relatively large transition strengths, and the close doublets (e.g. 2.68 and 2.72 MeV levels) were assumed to have different spins. The spectroscopic factor sums obtained in this way are 1.05 and 1.19, respectively.

The unperturbed single-particle energies E(J) may be estimated using the relation $E(J) = \Sigma_i E_i S_i / \Sigma_i S_i$, where the sums are over all levels of the same J. The values obtained using the spectroscopic factors of table 2.2 are $E(\frac{1}{2}) = 2.67$ MeV and $E(\frac{3}{2}) = 0.99$ MeV, hence the $2p_{1/2} - 2p_{3/2}$ spacing $\Delta = 1.68$ MeV in good agreement with the single-particle energy difference of 2.03 MeV found for ^{49}Ca in ref.[64]).

Of particular interest is the spin of the 3.61 MeV level. The earlier γ-γ correlation experiment[63]), while not conclusive, tended to favour a spin of $\frac{3}{2}$ for this state. This assignment appears to be supported by the lack of a dip in the ^{52}Cr(d,p) cross section leading to this level. However, DW calculations

show that for reactions with relatively small Q-values ($\lesssim$2 MeV), the dependence of the cross section on j is much reduced, therefore the Lee-Schiffer criterion ceases to be valid. This can be understood in terms of a decreasing contribution from the nuclear interior where the deuteron and proton spin-orbit forces are important. Thus the j-dependence rule should only be applied to ℓ = 1 transitions having Q values $\gtrsim$ 2 MeV. The vector analysing power measurements[36,37]) give a spin of $\frac{1}{2}$ for the 3.61 MeV state. This value is supported by the spectroscopic strengths of table 2.2 since the assumption of $\frac{3}{2}$ leads to poor results for both the spectroscopic factor sums and the spacing Δ.

2.3 The $^{50}Cr(d,p)^{51}Cr$ reaction

2.3.1 DW Analysis

The reaction $^{50}Cr(d,p)^{51}Cr$ has been studied by several workers[41-43,64]) at bombarding energies between 6 and 10 MeV. In the most extensive measurements, Robertshaw et al[43]) resolved the levels at 0.748 and 0.775 MeV in ^{51}Cr by using a multiple-gap spectrograph and observed about 20 ℓ = 1 transitions up to an excitation energy of 7.9 MeV (table 2.3). Of particular interest is the strong transition to the 1.895 MeV state. The j-dependence rule gives a definite J = $\frac{1}{2}$ assignment for this level at both 7.5 and 9.15 MeV[42]) (although at 10 MeV, the situation[41]) is less clear), while the γ-γ correlation work[58]) seems to rule out this possibility.

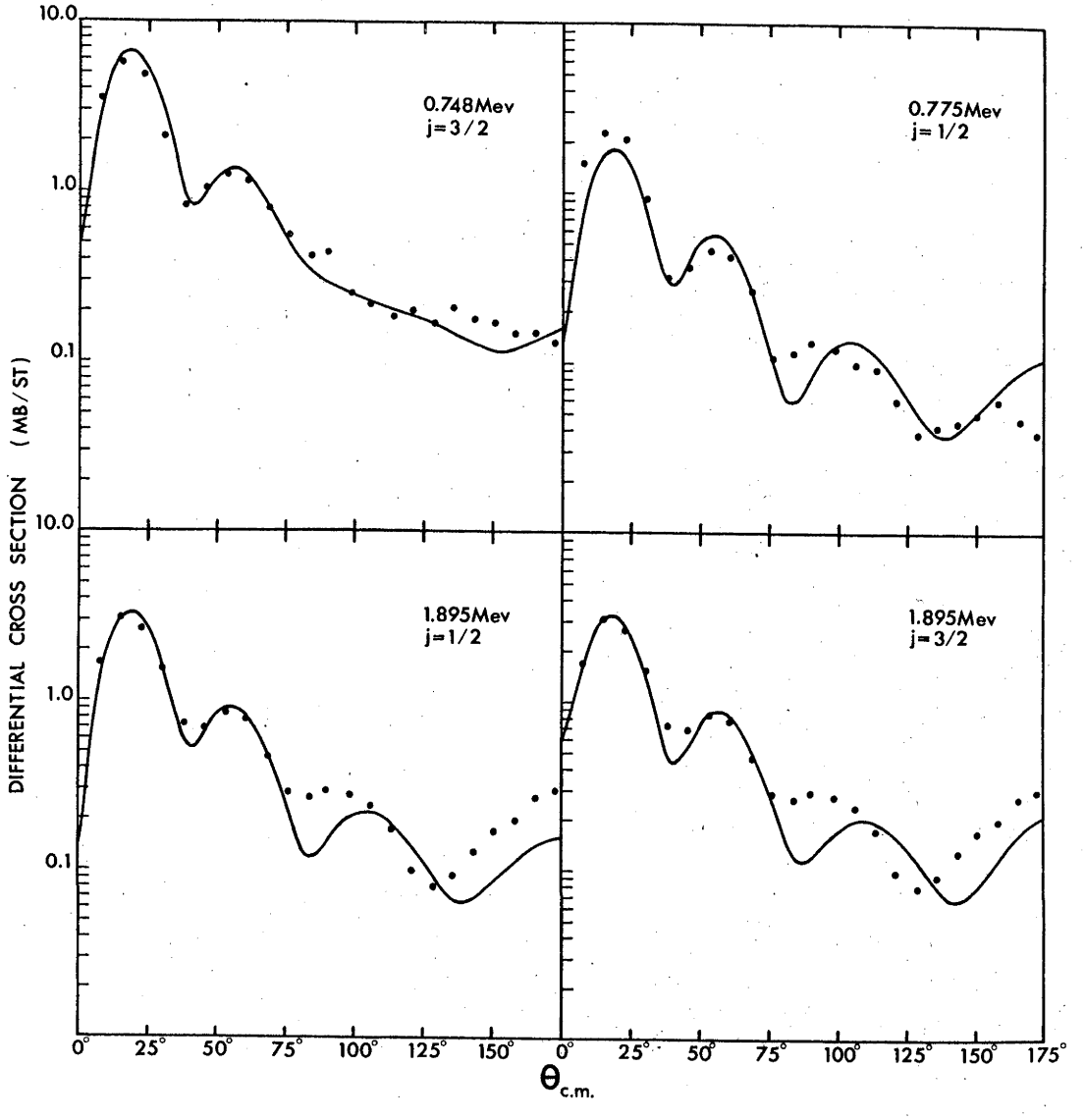

Fig. 2.3. Differential cross sections for the reaction $^{50}Cr(d,p)^{51}Cr$ leading to the 0.748, 0.775 and 1.895 MeV states in ^{51}Cr at 7.5 MeV bombarding energy. The solid curves are distorted wave calculations for the parameters of Table 2.1 and the points are the data of ref.[43]).

Table 2.3

SPECTROSCOPIC FACTORS FOR THE $^{50}Cr(d,p)^{51}Cr$ REACTION

Level E_x(MeV)	Q (MeV)	(2J+1)S	$J^{c)}$	S $J = \frac{1}{2}$	S $J = \frac{3}{2}$
0.748	6.293	1.89[a)]	$\frac{3}{2}$	-	0.47
0.775	6.266	0.55[a)]	$\frac{1}{2}$	0.28	-
1.895	5.146	0.66[a)]	$\frac{3}{2}$	-	0.17
2.887	4.154	0.38[a)]	$\frac{3}{2}$	-	0.09
3.054	3.987	0.11[a)]	$(\frac{1}{2})$	0.05	-
3.124	3.917	0.67[a)]	$\frac{3}{2}$	-	0.17
3.767	3.274	0.30[a)]	$\frac{3}{2}$	-	0.08
4.036	3.005	0.45[a)]	$(\frac{1}{2})$	0.23	-
4.426	2.615	0.05[b)]	$(\frac{3}{2})$	-	0.01
4.439	2.602	0.11[b)]	$(\frac{1}{2})$	0.05	-
4.684	2.357	0.04[b)]	$(\frac{3}{2})$	-	0.01
4.769	2.272	0.25[b)]	$(\frac{1}{2})$	0.13	-
5.202	1.839	0.19[b)]	$(\frac{3}{2})$	-	0.05
5.663	1.378	0.32[b)]	$(\frac{1}{2})$	0.16	-
5.741	1.300	0.12[b)]	$(\frac{1}{2})$	0.06	-
5.769	1.272	0.04[b)]	$(\frac{3}{2})$	-	0.01
5.952	1.089	0.06[b)]	$(\frac{1}{2})$	0.03	-
6.236	0.805	0.04[b)]	$(\frac{3}{2})$	-	0.01
6.360	0.681	0.08[b)]	$(\frac{1}{2})$	0.04	-
7.206	-0.165	0.03[b)]	$(\frac{1}{2})$	0.01	-
	Sum	6.34		1.04	1.07

[a)] present work [b)] ref.[43] [c)] Tentative spin assignments are indicated in parentheses. Preferred values are partially arbitrary and partially based upon $2p_{1/2}$ and $2p_{3/2}$ sum rules and shell model systematics.

In order to investigate this discrepancy for the 1.895 MeV state, DW calculations as discussed in the previous section were carried out for the transitions to the 0.748, 0.775 and 1.895 MeV levels. The spins of the doublet states are known[58]) to be $\frac{3}{2}$ and $\frac{1}{2}$ respectively and fig. 2.3 shows that these assignments are in agreement with the j-dependence criterion. The angular distributions for these two states can be qualitatively described using OM parameters which are similar (but not identical) to those employed for the $^{52}Cr(d,p)^{53}Cr$ reaction. Fig. 2.3 shows the predictions for the parameters of table 2.1. Only the deuteron and proton real central potentials V were varied in the fitting procedure. It is probable that the required changes in V could be reduced by allowing other parameters to vary simultaneously. The 8 MeV modification in the deuteron well depth appears to be partly a reflection of the different Q-values of the respective reactions. It seems that the optimum value of the deuteron potential V (the other parameters being unchanged) decreases as the Q-value of the reaction diminishes. Indeed, a better fit to the $^{52}Cr(d,p)^{53}Cr$ (3.61 MeV state) can be obtained by using $V < 100$ MeV, and a similar analysis[44]) of some $^{54}Cr(d,p)^{55}Cr$ data (g.s. Q = 4.03 MeV) requires V = 95 MeV.

If the same parameters obtained by fitting the doublet states are used for the 1.895 MeV transition, a $J = \frac{1}{2}$ spin assignment is unamibuously determined from the analysis. This is to be expected since the calculated cross sections vary slowly with the Q-value of the reaction, and both the 0.775 and 1.895 MeV

angular distributions exhibit a dip near 125° (fig. 2.3). However, an equally good fit to the 1.895 MeV cross section is obtained for J = $^3/_2$ if the deuteron potential V is increased to 120 MeV. This means that the violation of the j-dependence rule for the 1.895 MeV transition may be interpreted as arising from unusually large corrections of the form discussed earlier. An alternative explanation, i.e. the occurrence of a close doublet at 1.895 MeV having spins $^1/_2$ and $^3/_2$, respectively, appears unlikely.

2.3.2 Spectroscopic Factors

Spectroscopic strengths (2J+1)S were obtained for the eight ℓ = 1 transitions up to an excitation energy of 4.036 MeV by normalizing the zero-range DW predictions multiplied by a FR correction factor of 1.65 against the experimental data to obtain an overall best fit. The results are given in table 2.3 in which the corresponding strengths for the higher levels are taken from a previous analysis[43]). The sum of the strengths is 6.3, which agrees very well with the expected value of 6.0 for the simple shell model.

The spins of several of the lower states have been determined[58]), namely J = $^3/_2$ for the 0.748, 1.895, 2.887, 3.124 and 3.767 MeV states and J = $^1/_2$ for the 0.775 MeV level. The other states were assumed to have the spins given in table 2.3 (in parentheses). These values are partially arbitrary and partially based upon the $2p_{1/2}$ and $2p_{3/2}$ sum rules and shell-model systematics as in the case of ^{53}Cr. The spectroscopic factor sums obtained

in this manner are close to the full single-particle strength of unity.

The unperturbed single-particle energies in ^{51}Cr were estimated to be E($\frac{1}{2}$) = 3.72 MeV and E($\frac{3}{2}$) = 2.08 MeV, respectively, giving a spacing Δ = 1.64 MeV. This value of Δ is in good agreement with the values of 1.68 MeV and 1.66 MeV (ref.[44])) for ^{53}Cr and ^{55}Cr, respectively. If the spin of the 1.895 MeV level is taken to be $\frac{1}{2}$, either the $2p_{\frac{1}{2}}$ and $2p_{\frac{3}{2}}$ spectroscopic sum rules are substantially different (it is assumed that the ℓ = 1 transitions belong to the 2p shell) or the spacing Δ is significantly decreased. These considerations therefore favour a $\frac{3}{2}$ assignment for the 1.895 MeV level.

2.4 Conclusions

The j-dependence of several ℓ = 1 transitions in the ^{50}Cr(d,p) and ^{52}(d,p) reactions at 7.5 and 8 MeV deuteron bombarding energy respectively, has been qualitatively described using the DW theory. This was only achieved by allowing the deuteron OM parameters to be rather different from those which describe the corresponding elastic scattering measurements. This implies that the theoretical description is not strictly valid, and that the different potentials are required to partially compensate for deficiencies in the models. A recent investigation[65]) indicates that such a difference in the deuteron parameters is to be expected.

A j-dependence rule, such as the Lee-Schiffer criterion, may exist when the corrections for each transition produce a similar modification to the deuteron potential so that essentially the same parameters are appropriate for each level (although the optimum value of the deuteron well depth V(the other parameters being unchanged) decreases as the Q-value of the reaction diminishes). In this case the angular distributions for $j = \frac{1}{2}$ and $j = \frac{3}{2}$ transitions will be systematically different at backward angles; the difference arises as a consequence of the deuteron and proton spin-orbit interactions. The calculations indicate that for reactions with relatively small Q values ($\lesssim 2$ MeV), the j-effect is much reduced so that the Lee-Schiffer criterion ceases to be valid. This is the result of a decreasing contribution from the nuclear interior where the deuteron and proton spin-orbit forces are important.

The reaction $^{50}Cr(d,p)^{51}Cr$ (1.895 MeV state) exhibits a violation of the j-dependence rule probably because the corrections in this case are unusually large and thus the optimum deuteron parameters for the DW calculation are considerably different from the average values. A spin assignment of $\frac{3}{2}$ for the 1.895 MeV level in ^{51}Cr is supported by the present investigation.

The $2p_{\frac{1}{2}}$ and $2p_{\frac{3}{2}}$ spectroscopic factor sums obtained are in good agreement with the simple shell model, and the unperturbed single-particle level spacings were estimated to be between 1.6 and 1.7 MeV for both ^{51}Cr and ^{53}Cr.

CHAPTER 3

EFFECT OF TENSOR FORCES IN THE DEUTERON OPTICAL POTENTIAL

3.1 Introduction

Several measurements of the tensor polarizations of deuterons elastically scattered by ^{27}Al, ^{28}Si and ^{60}Ni (ref.[66]), ^{12}C (ref.[67]) and ^{40}Ca (ref.[52]) have been carried out at bombarding energies between 3.5 and 11 MeV. These data have been analysed in terms of the OM to determine whether possible tensor forces[2]) in the deuteron-nucleus interaction are negligible or not. Schwandt and Haeberli[52,66]) found that better fits to the measured $\langle T_{20} \rangle$ and $\langle T_{22} \rangle$ tensor moments can be obtained if either a long-ranged attractive T_R (ref.[67]) tensor force or a short-ranged repulsive T_L tensor interaction is included separately in the optical potential. However, the T_L term has a detrimental effect on the fits to the corresponding cross sections and vector polarizations, therefore the T_R potential is more acceptable over-all. In the work of Cords et al[67]), both tensor terms were used simultaneously to describe $\langle T_{20} \rangle$, $\langle T_{21} \rangle$ and $\langle T_{22} \rangle$ polarizations, but further studies[68,69]) indicate that the T_L tensor is redundant.

This chapter presents a study of the effect of the tensor forces T_R and T_L on the DW predictions for deuteron stripping reactions and in particular an investigation of the j-dependence of the cross-sections[46]) and vector analysing powers[36,37]). In

view of the slowness of the computations, calculations were performed for only two representative examples of j-dependence in the differential cross section, namely $\ell = 1$ transitions in the reaction $^{40}Ca(d,p)^{41}Ca$ leading to the 2.47 MeV ($\frac{3}{2}^-$) and 3.95 MeV ($\frac{1}{2}^-$) levels. The essential features of these cross sections and vector analysing powers have been described[36,51,52]) using the DW theory without any tensor forces in the deuteron optical potential, thus the effects of such tensor interactions in these cases are probably small. The calculations of this chapter show that including a T_R tensor force which is compatible with the elastic scattering data has no significant effect on the cross sections or vector analysing powers. The changes in the corresponding proton polarizations and deuteron tensor analysing powers are also evaluated; for completeness, the variations resulting from a small T_L tensor term are included.

3.2 Results and discussion

Calculations were carried out for the reaction $^{40}Ca(d,p)^{41}Ca$ leading to the 2.47 MeV ($\frac{3}{2}^-$) and 3.95 MeV ($\frac{1}{2}^-$) residual states at 9 MeV deuteron bombarding energy. The OM parameters for the central and spin-orbit interactions, which were kept constant throughout the DW computations, are given in table 3.1. The deuteron potential was obtained by Satchler[70]) by fitting both elastic scattering cross section data[52,71]) and polarization measurements[52]) assuming no tensor forces. The proton and neutron parameters were taken close to conventional values.

Table 3.1

POTENTIALS

	Deuteron	Proton	Neutron
V (MeV)	94.1	45.0	adjusted
r_V (fm)	1.177	1.250	1.250
a_V (fm)	0.798	0.650	0.650
W (MeV)	10.0	7.0	
r_W (fm)	1.602	1.250	
a_W (fm)	0.472	0.47	
S (MeV fm^2)	17.9	16.0	
r_S (fm)	0.780	1.250	
a_S (fm)	0.520	0.650	
r_C (fm)	1.250	1.250	

In the present work, typical values of the radius and diffuseness parameters, r_R = 1.4 fm, a_R = 0.7 fm, r_L = 0.7 fm and a_L = 0.4 fm were chosen for the tensor potentials. Fig. 3.1 shows the variations in the differential cross section and proton polarization for the j = ½ 3.95 MeV transition which occur when either a small T_R or a small T_L tensor interaction is included separately in the deuteron-nucleus optical potential. The proton polarization is a vector polarization analogous to $\langle iT_{11} \rangle$ for deuterons and in this chapter is taken as $\frac{\sqrt{2}}{2}$ times the usual polarization (Basel convention).

The magnitudes of the tensor terms |M| = 2 MeV and |Q| = 1 MeV are approximately one-half of the strengths found by Schwandt and Haeberli[52]) to give a better description of elastic deuteron tensor polarizations. Figs. 3.2 and 3.3 show similar changes for the deuteron vector and tensor analysing powers. The equivalence between analysing powers and polarizations has been discussed in Chapter 1. Figs. 3.4 and 3.5 show corresponding results for the j = ³⁄₂ 2.47 MeV transition.

It is seen that T_R has very little effect on the cross sections, proton polarizations or deuteron vector analysing powers but does significantly change two of the tensor analysing powers, e.g. $\langle T_{20} \rangle$ and $\langle T_{21} \rangle$ in the case of the j = ½ transition. On the other hand, T_L has a large effect on all the quantities for angles greater than about 60^0. It was found that providing the variations are small, the changes are roughly proportional to the strengths of the tensor potentials and are on either side of the

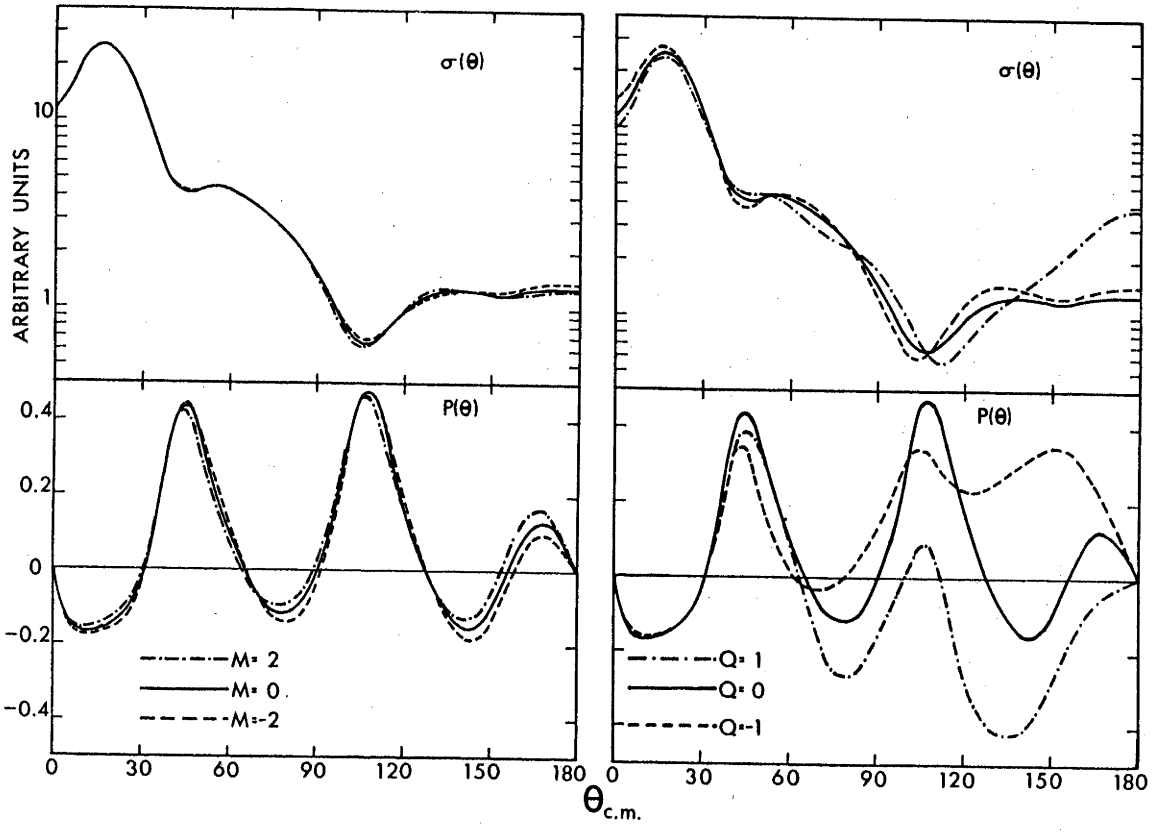

Fig. 3.1. Differential cross section and proton polarization for the reaction $^{40}Ca(d,p)^{41}Ca$ (3.95 MeV state) at 9 MeV bombarding energy. The curves are predictions of the distorted wave theory for the parameters of Table 3.1 and the inclusion of either a T_R or T_L tensor potential respectively.

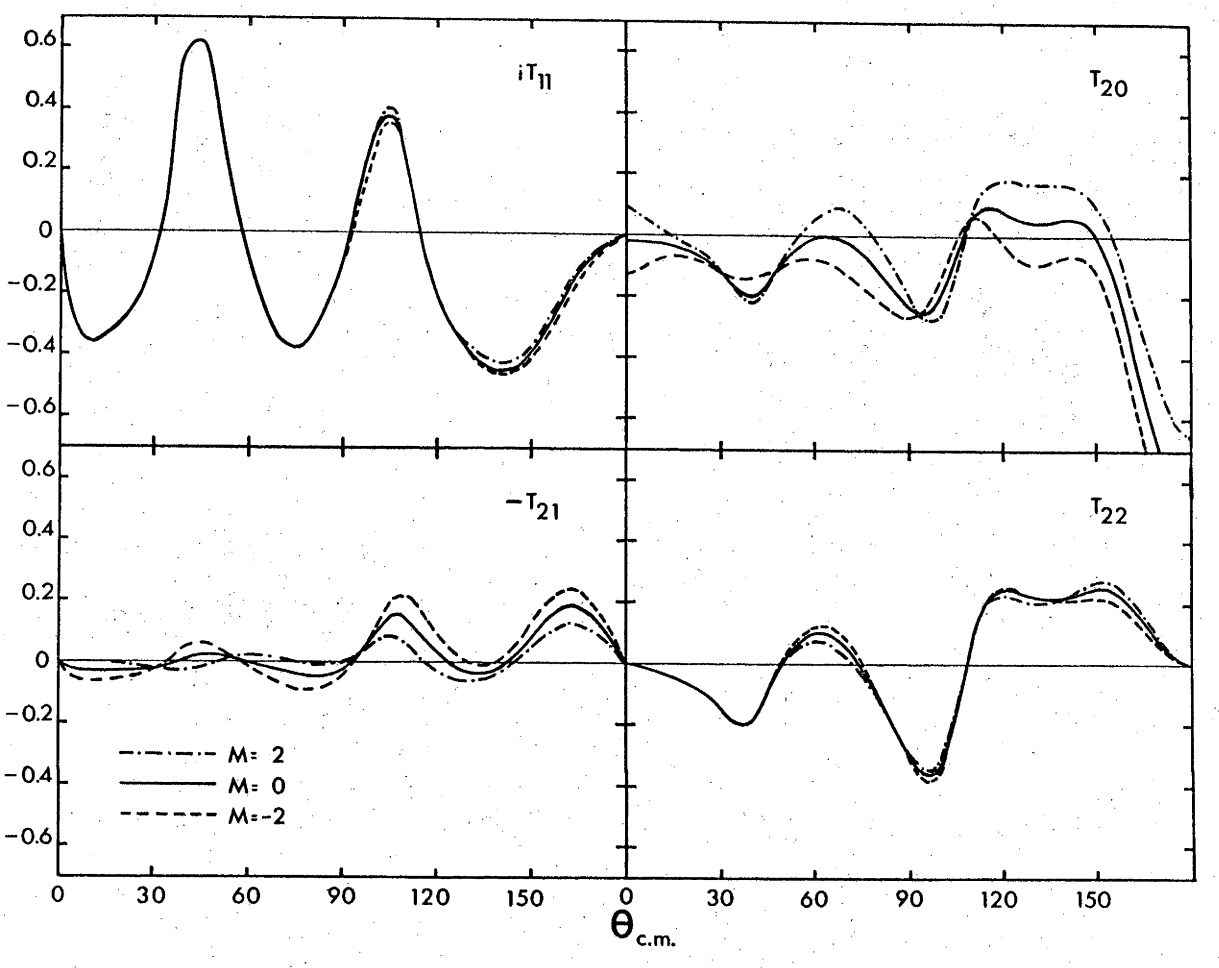

Fig. 3.2. Deuteron vector and tensor analysing powers for the reaction $^{40}Ca(d,p)^{41}Ca$ (3.95 MeV state) at 9 MeV bombarding energy. The curves are predictions of the distorted wave theory for the parameters of Table 3.1 and the inclusion of a tensor term T_R.

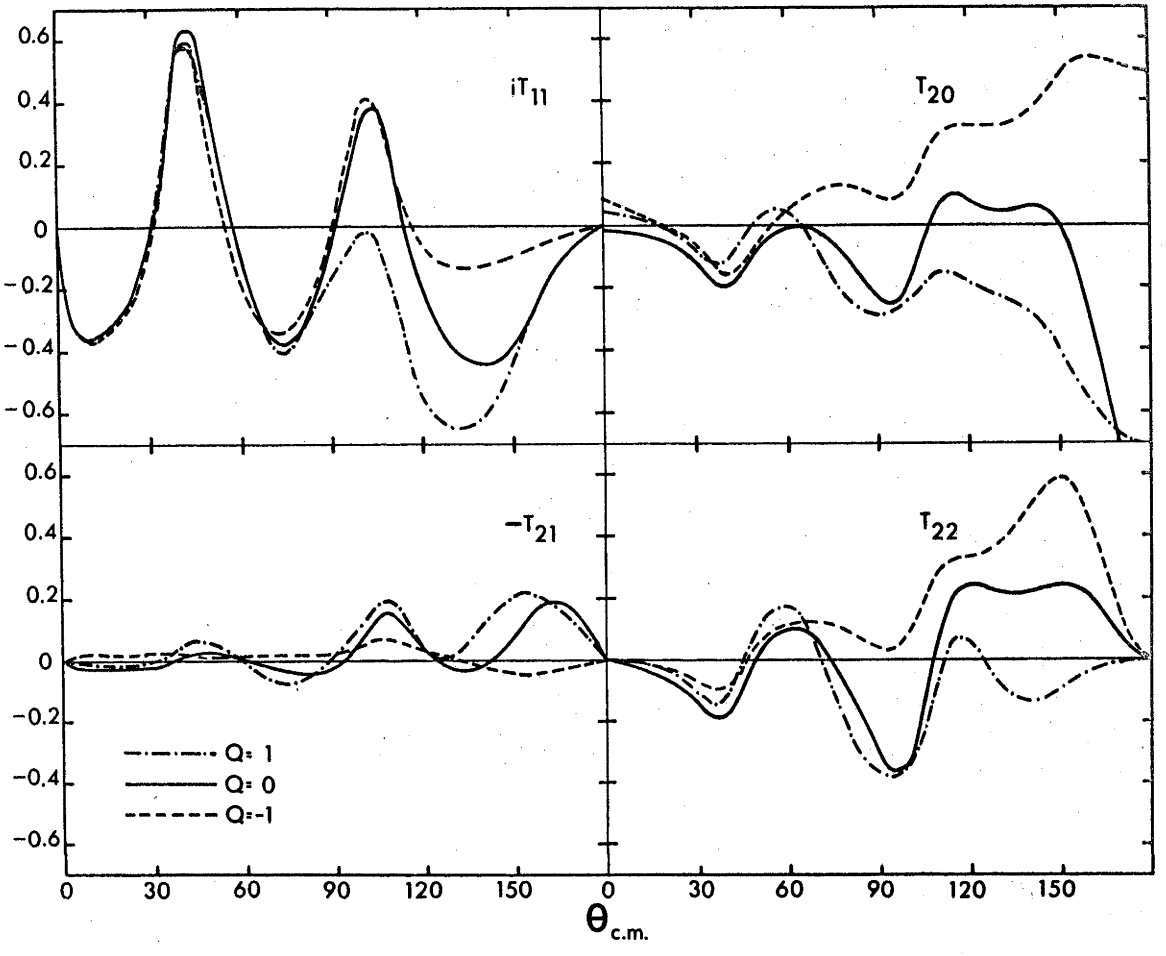

Fig. 3.3. Deuteron vector and tensor analysing powers for the reaction $^{40}Ca(d,p)^{41}Ca$ (3.95 MeV state) at 9 MeV bombarding energy. The curves are predictions of the distorted wave theory for the parameters of Table 3.1 and the inclusion of a tensor term T_L.

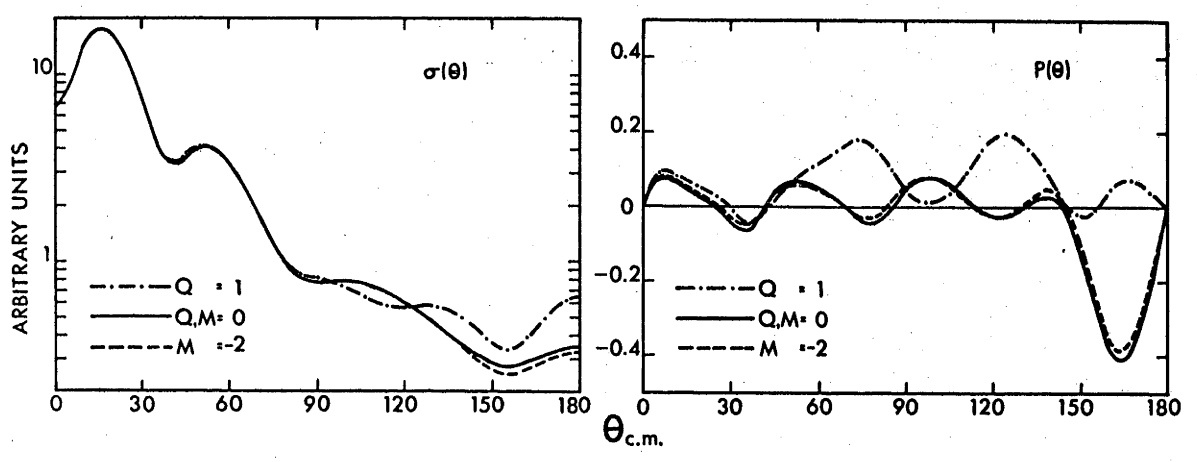

Fig. 3.4. Differential cross section and proton polarization for the reaction $^{40}Ca(d,p)^{41}Ca$ (2.47 MeV state) at 9 MeV bombarding energy. The curves are predictions of the distorted wave theory for the parameters of Table 3.1 and the inclusion of either a T_R or T_L tensor potential respectively.

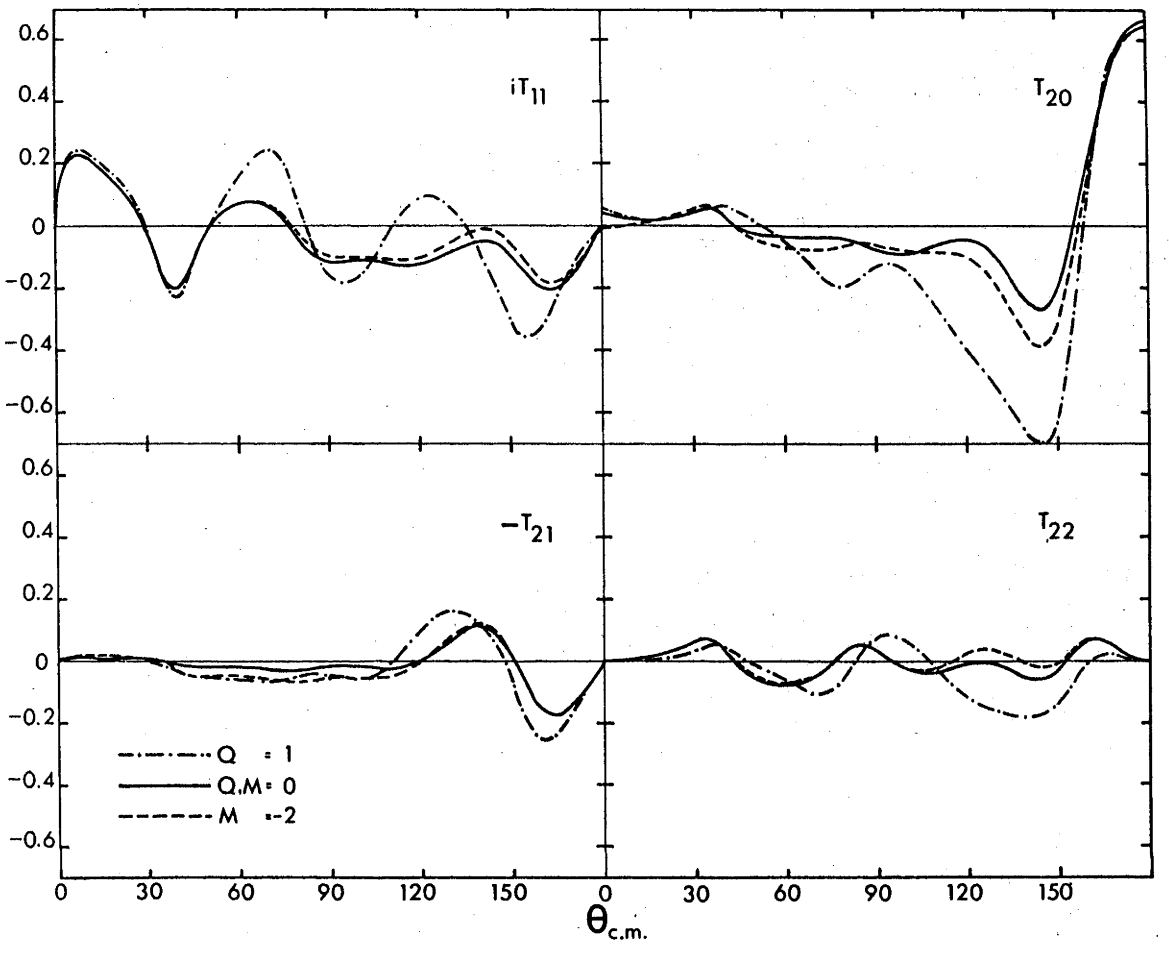

Fig. 3.5. Deuteron vector and tensor analysing powers for the reaction $^{40}Ca(d,p)^{41}Ca$ (2.47 MeV state) at 9 MeV bombarding energy. The curves are predictions of the distorted wave theory for the parameters of Table 3.1 and the inclusion of either a T_R or T_L tensor potential.

M = Q = 0 curves depending whether the interaction is attractive or repulsive. The j-dependence of the deuteron vector analysing powers at forward angles is not significantly affected by the introduction of either the T_R or T_L tensor term. On the other hand, the j-dependence of the corresponding cross sections is a large-angle effect and will be modified if the T_L tensor is not too small. However, it appears unlikely that a T_L potential, which is compatible with elastic scattering data, will affect the qualitative behaviour of the j-dependence of those (d,p) cross sections which resemble the cases studied here.

3.3 Conclusions

The inclusion of a small tensor interaction T_R in the deuteron optical potential, which gives a better description of elastic scattering polarization measurements, does not significantly affect the cross sections, proton polarizations and deuteron vector analysing powers for the $\ell = 1$ transitions in the reaction $^{40}Ca(d,p)^{41}Ca$ leading to the 2.47 MeV ($\frac{3}{2}^-$) and 3.95 MeV ($\frac{1}{2}^-$) levels. The corresponding tensor analysing powers $\langle T_{20} \rangle$ and $\langle T_{21} \rangle$ but not $\langle T_{22} \rangle$ are considerably changed in the case of the $j = \frac{1}{2}$ transition. On the other hand, a relatively small T_L tensor potential, presumably because of its quadratic dependence or orbital angular momentum, does lead to significant changes in all the quantities at backward angles. Consequently, the j-dependent effects are practically unchanged when a small T_R term is introduced but are considerably modified at backward angles even for a relatively small T_L potential.

CHAPTER 4

EXACT FINITE-RANGE CALCULATIONS INCLUDING THE D-STATE OF THE DEUTERON

4.1 Introduction

This chapter presents exact FR calculations which include the deuteron D-state for some $\ell = 1$ transitions in (d,p) and (p,d) reactions at several energies as follows:

i) $^{52}Cr(d,p)^{53}Cr$ to the $\frac{3}{2}^-$ g.s. and $\frac{1}{2}^-$ 0.57 MeV level in ^{53}Cr for 8 MeV incident deuteron energy (calculations with a small T_R tensor were also performed),

ii) $^{40}Ca(d,p)^{41}Ca$ to the 2.47 ($\frac{3}{2}^-$) and 3.95 MeV ($\frac{1}{2}^-$) levels in ^{41}Ca at 7 and 9 MeV incident deuteron energies,

iii) $^{16}O(p,d)^{15}O$ to the g.s. ($\frac{1}{2}^-$) and 6.18 MeV ($\frac{3}{2}^-$) level in ^{15}O at 25.52, 30 and 31.82 MeV incident proton energies.

It was of interest to determine if the D-state effects are functions of reaction parameters such as target mass, Q-value, deuteron bombarding energy or OM parameters and also to compare spectroscopic factors predicted by FR and ZR calculations. The main aims, however, were to investigate the effect of the D-state

upon (a) the j-dependence of the differential cross sections and the deuteron vector analysing powers[36-39]) and proton polarizations[38,72])for typical ℓ = 1 transitions and (b) the corresponding tensor analysing powers.

4.2 The $^{52}Cr(d,p)^{53}Cr$ reaction

Calculations based on the theoretical formulation of chapter 1 are presented for the reaction $^{52}Cr(d,p)^{53}Cr$ leading to the ground ($\frac{3}{2}^-$) and 0.57 MeV ($\frac{1}{2}^-$) residual states at 8 MeV deuteron bombarding energy. The OM parameters for the central and spin-orbit interactions were taken from an earlier analysis of the same reactions[73]) (see table 2.1).

The results for the differential cross sections are shown in fig. 4.1 and it is seen that the shapes of the angular distributions are very similar to the corresponding ZR calculations. The FR curves (S+D) lie below the ZR cross sections when D_0^2 is assumed to have the value 1.65×10^4 MeV^2 fm^3 (ref.[21])). Normalizing the ZR calculation to the FR curve at the first peak for the g.s. and 0.57 MeV state gives D_0^2 = 1.42 and 1.46×10^4 MeV^2 fm^3, respectively. The effect of including a small tensor term T_R (M = -4 MeV, r_R = 1.4 fm and a_R = 0.7 fm (ref.[53]), see ch. 3)) in the deuteron-nucleus interaction (curve S+D+T_R) or neglecting the D-state of the deuteron (curve S) is negligible. Thus, for these cases, the inclusion of the D-state has an insignificant effect upon the j-dependence of the angular distributions.

Figs. 4.2 and 4.3 show the corresponding results for the

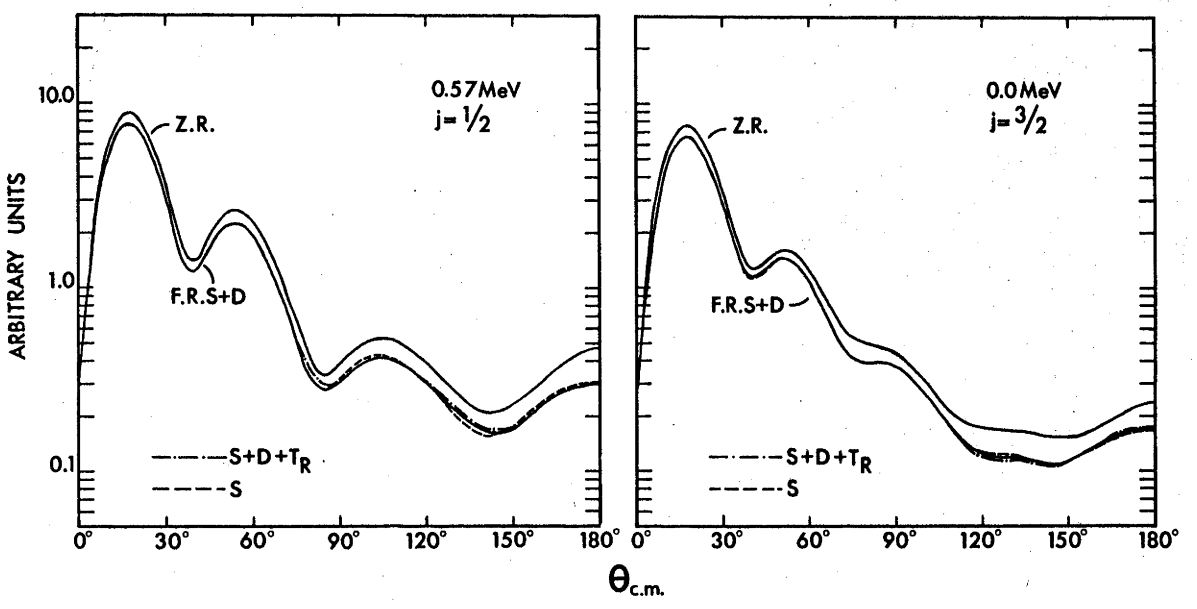

Fig. 4.1. Differential cross sections for the reaction $^{52}Cr(d,p)^{53}Cr$ leading to the 0.57 MeV and ground states in ^{53}Cr at 8 MeV bombarding energy. The upper solid curves are the usual ZR calculations with $D_0^2 = 1.65 \times 10^4 MeV^2 fm^3$ and the lower solid curves are the D-state FR predictions. The effect of including a small tensor interaction or neglecting the D-state of the deuteron is indicated by curves ($S+D+T_R$) or (S), respectively.

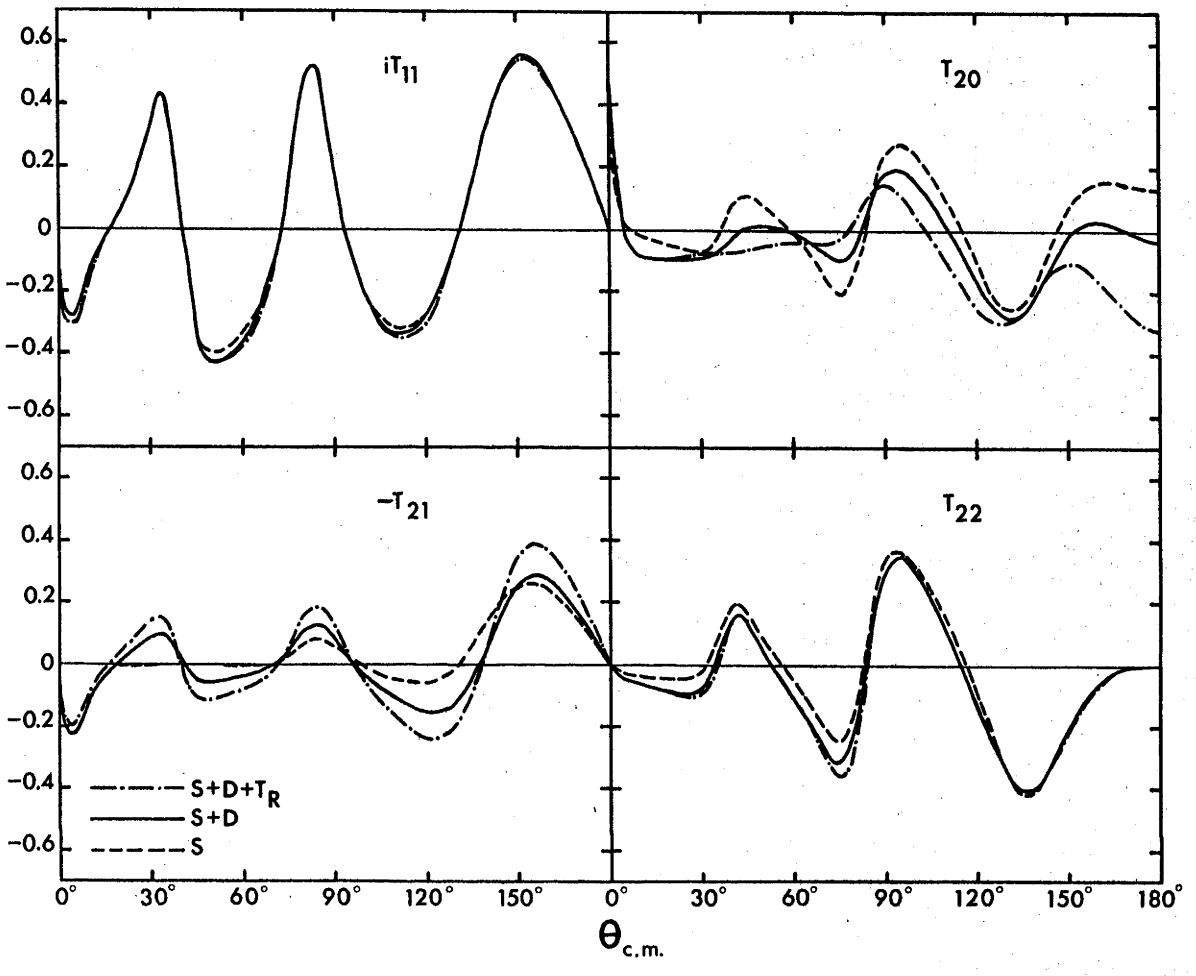

Fig. 4.2. Deuteron vector and tensor analysing powers for the reaction $^{52}Cr(d,p)^{53}Cr$ (0.57 MeV state) at 8 MeV bombarding energy. The full curves are the D-state FR predictions. The effect of including a small tensor interaction or neglecting the D-state of the deuteron is indicated by curves ($S+D+T_R$) or (S), respectively.

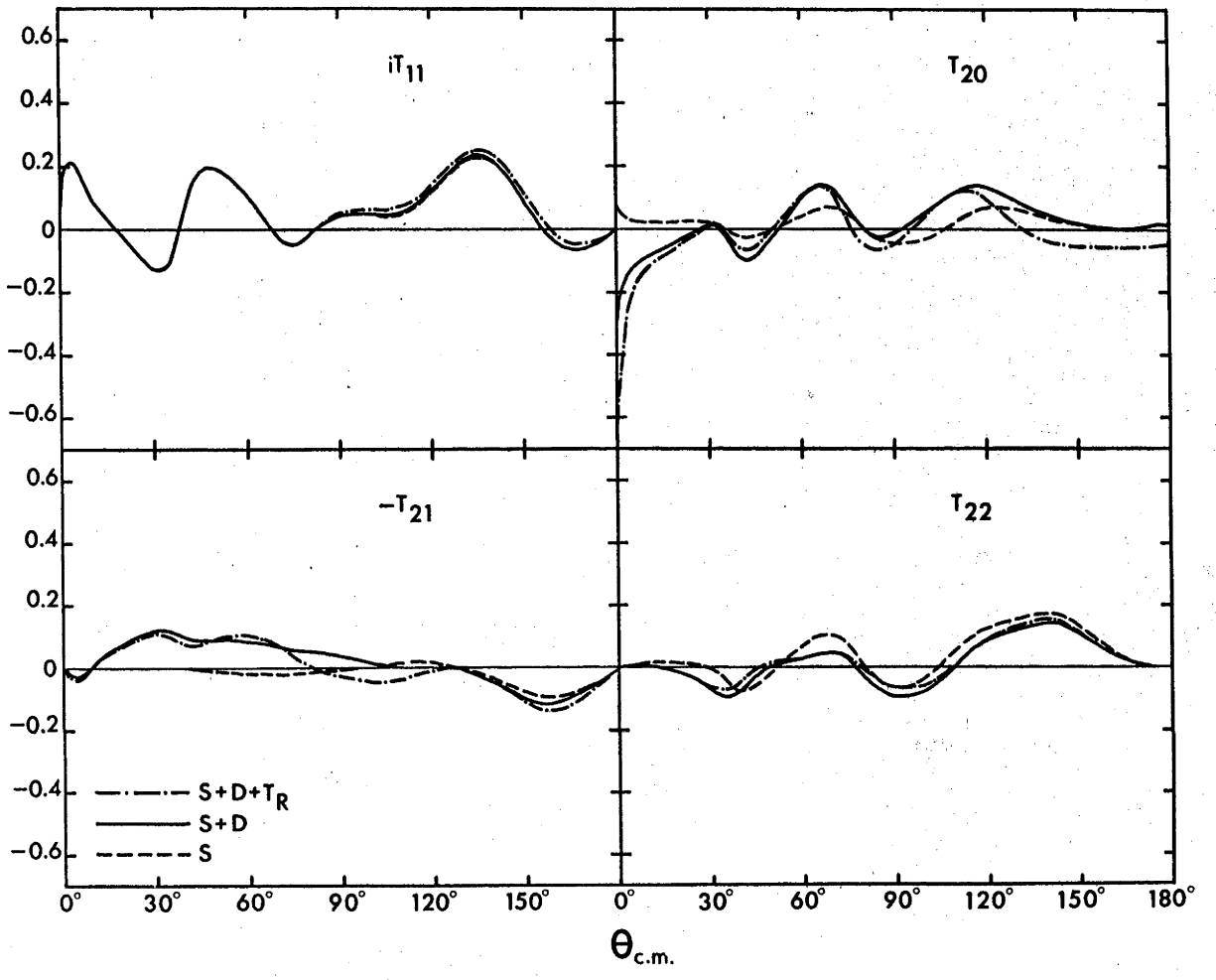

Fig. 4.3. Deuteron vector and tensor analysing powers for the reaction $^{52}Cr(d,p)^{53}Cr$ (g.s.) at 8 MeV bombarding energy. The full curves are the D-state FR predictions. The effect of including a small tensor interaction or neglecting the D-state of the deuteron is indicated by curves ($S+D+T_R$) or (S), respectively.

vector and tensor analysing powers referred to the coordinate system defined in chapter 1. The ZR predictions lie close to the curves labelled S and for simplicity have been omitted from the diagrams. It is seen that the vector analysing powers are practically insensitive to the deuteron D-state. However, the tensor analysing powers, especially $\langle T_{20} \rangle$ and $\langle T_{21} \rangle$ are significantly modified by the inclusion of firstly, the D-state (curves S+D) and then the tensor interaction as well (curves $S+D+T_R$). The effect of T_R is larger for the $j = \frac{1}{2}$ transition in agreement with the previous work[53]) of chapter 3 but is smaller than the D-state contribution for both reactions.

4.3 The $^{40}Ca(d,p)^{41}Ca$ reaction

Several studies of the reaction $^{40}Ca(d,p)^{41}Ca$ in the ZR[4,36,50-52]) and FR[4]) formulations of the DWBA have described j-dependent features of the cross sections and vector analysing powers[36,37]) for several strong $\ell = 1$ transitions and also (in chapter 3) the effect of a small tensor term in the deuteron-nucleus optical potential[53]). Here calculations are reported for two $\ell = 1$ transitions leading to the 2.47 ($\frac{3}{2}^-$) and 3.95 MeV ($\frac{1}{2}^-$) levels (Q = 3.67 and 2.19 MeV respectively) at 7 and 9 MeV deuteron bombarding energies using the OM parameters of table 4.1. The deuteron parameters at 7 MeV (part of a set which varies smoothly as a function of energy) are the result of an extensive elastic scattering analysis[52]) and led to good fits to the 7 MeV cross section and vector polarization data. The 9 MeV deuteron

Table 4.1

POTENTIALS FOR $^{40}Ca(d,p)^{41}Ca$

E_d (MeV)	Deuteron		Proton[c]		Neutron
	7[a]	9[b]	7	9	
V (MeV)	110.5	94.1	53.8	53	adjusted
r_V (fm)	1.05	1.177	1.17	1.17	1.25
a_V (fm)	0.85	0.798	0.75	0.75	0.65
W (MeV)	10	10	9.6	9	
r_W (fm)	1.64	1.602	1.32	1.32	
a_W (fm)	0.529	0.472	0.527	0.527	
S (MeV fm^2)	18	17.9	12.4	12.4	
r_s (fm)	0.9	0.78	1.01	1.01	
a_s (fm)	0.6	0.52	0.75	0.75	
r_c (fm)	1.3	1.25	1.25	1.25	

a) ref.[52])

b) ref.[51,53])

c) ref.[74])

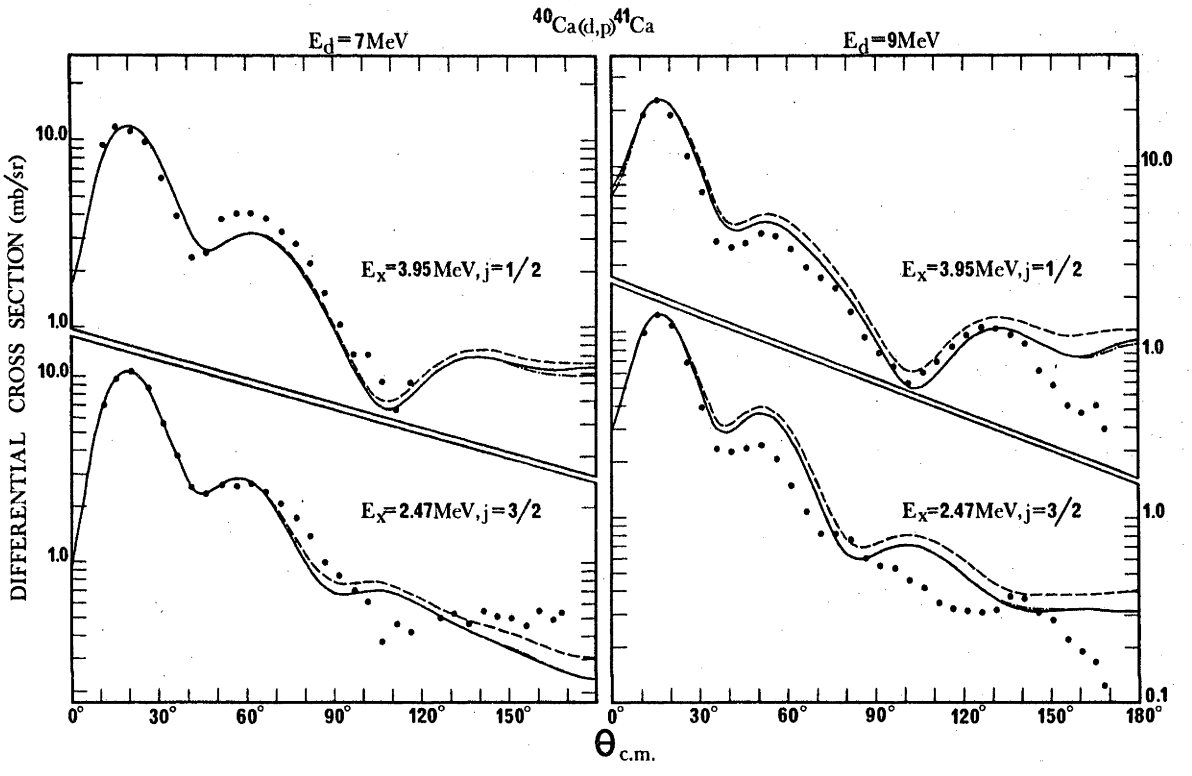

Fig. 4.4. Differential cross sections for the reaction $^{40}Ca(d,p)^{41}Ca$ leading to the 2.47 $\left(\frac{3}{2}^-\right)$ and 3.95 MeV $\left(\frac{1}{2}^-\right)$ states in ^{41}Ca at 7 and 9 MeV deuteron bombarding energies. The solid and dash-dot curves are the exact FR calculations with and without the D-state respectively and the broken curves the ZR predictions for the parameters of Table 4.1. The points are the data of ref.[4]).

Table 4.2

SPECTROSCOPIC FACTORS FOR THE REACTION $^{40}Ca(d,p)^{41}Ca$

E_d (MeV)	Q (MeV)	σ_{expt} (mb/sr)	σ_{th}(FRS+D) (mb/sr)	σ_{th}(ZR)[a]) (mb/sr)	S(FRS+D)	S(ZR)[a])
7	2.19	11.80	20.35	23.10	0.58	0.51
	3.67	10.70	29.43	33.71	0.36	0.32
9	2.19	22.80	29.16	33.10	0.78	0.69
	3.67	12.50	43.72	51.00	0.29	0.25

[a]) using $D_0^2 = 1.65 \times 10^4$ MeV^{2}fm^3

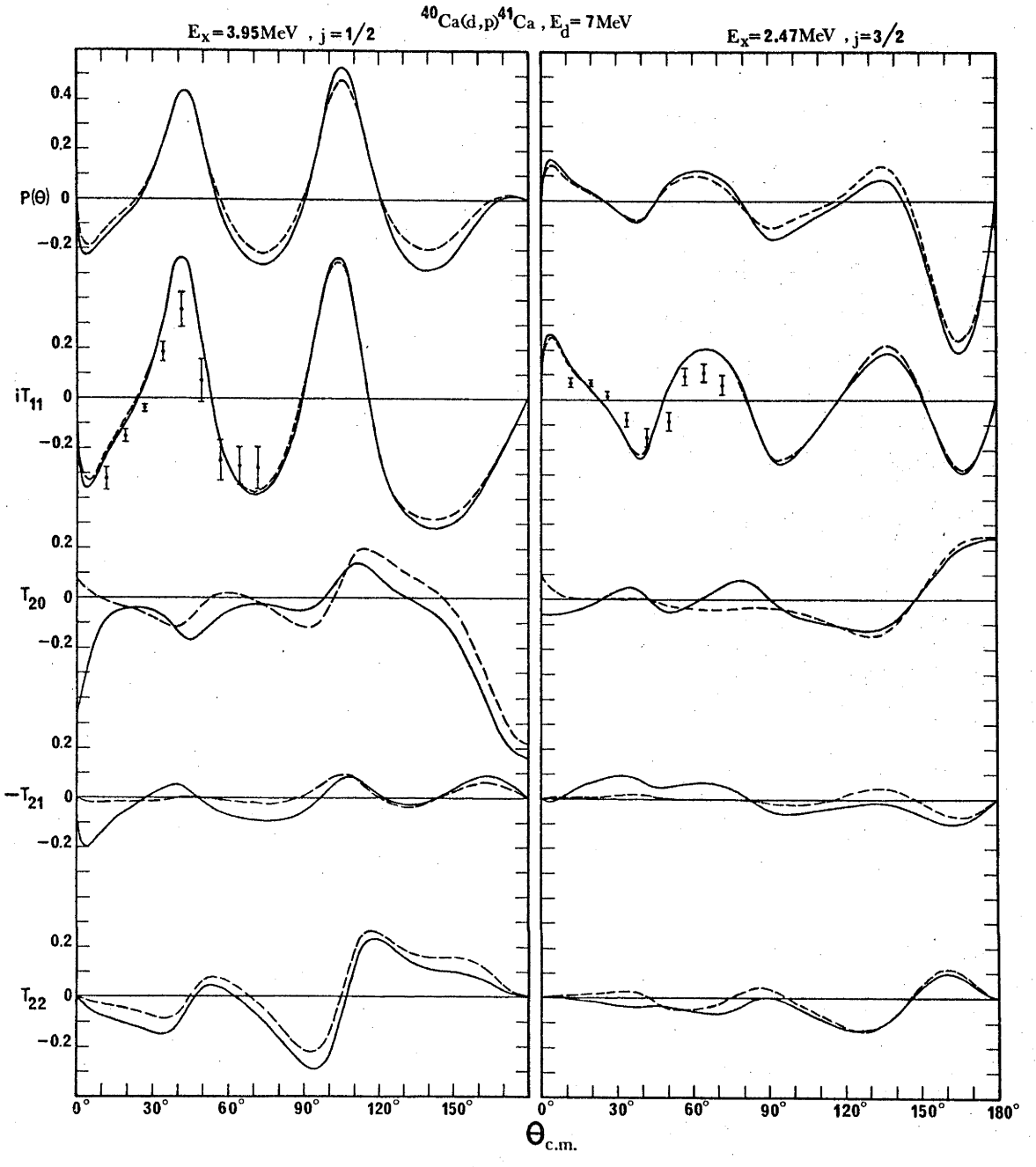

Fig. 4.5. Proton polarizations and deuteron analysing powers for the reaction ^{40}Ca(d,p)^{41}Ca (2.47 and 3.95 MeV states) at 7 MeV bombarding energy. The solid and broken curves are the exact FR S+D-state and ZR predictions respectively for the parameters of Table 4.1. The points are the data of ref.[36]).

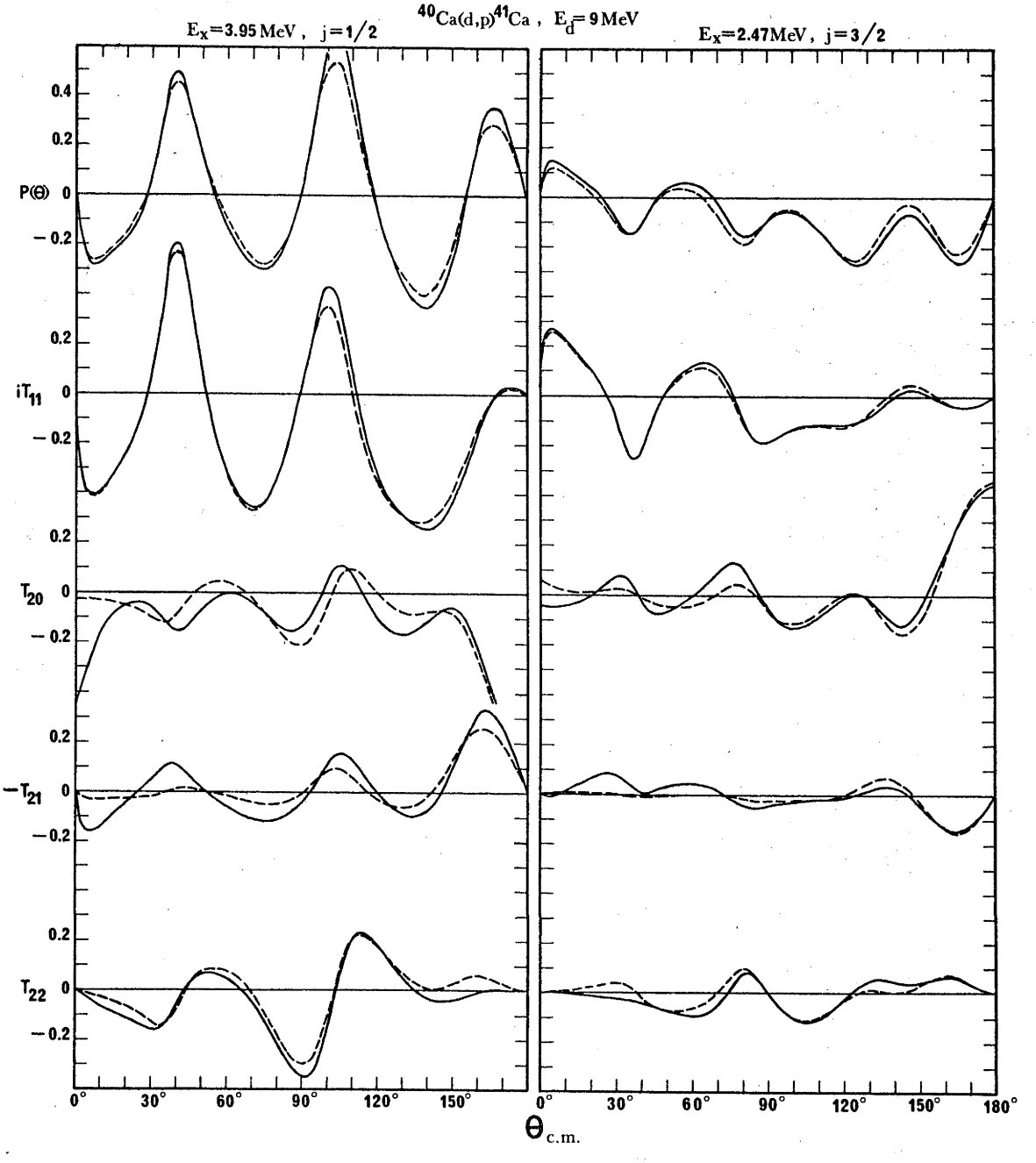

Fig. 4.6. Proton polarizations and deuteron analysing powers for the reaction ^{40}Ca(d,p)^{41}Ca (2.47 and 3.95 MeV states) at 9 MeV bombarding energy. The solid and broken curves are the exact FR S+D-state and ZR predictions respectively for the parameters of Table 4.1.

Figs. 4.5 and 4.6 show the corresponding proton polarizations $P(\theta)$ (defined according to the Basel convention) and the deuteron vector and tensor analysing powers $\langle iT_{11}\rangle$ and $\langle T_{2k}\rangle$ at deuteron bombarding energies of 7 and 9 MeV respectively. The data at 7 MeV are those of ref.[36]). For the sake of clarity the FR S-state calculations are not shown since they are very similar to the corresponding ZR predictions. The inclusion of the deuteron D-state affects $P(\theta)$ slightly more than it does $\langle iT_{11}\rangle$, but in general the effects are small for these two quantities hence j-dependent effects are unaltered while the corresponding deuteron tensor analysing powers are significantly changed. Here minimal differences exist between FR S-state and ZR and the effects apparent in $\langle T_{20}\rangle$, $\langle T_{21}\rangle$ (which otherwise is quite small for angles $\lesssim 70^0$) and to a lesser extent $\langle T_{22}\rangle$ are due to the D-state. Apart from variations in shape, the effects persist at 9 MeV and calculations at 12 MeV using two different elastic scattering parameter sets for the deuteron[52,75]) showed similar differences.

4.4 The $^{16}O(p,d)^{15}O$ reaction

Cross sections for the reaction $^{16}O(p,d)^{15}O$ for two $\ell = 1$ transitions leading to the g.s.($\frac{1}{2}^-$) and the 6.18 MeV ($\frac{3}{2}^-$) level in ^{15}O (Q = - 13.44 and - 19.62 MeV respectively) were measured by Chant et al[72]) at a proton bombarding energy of 30 MeV and by Snelgrove and Kashy[76]) at 21.27, 25.52, 31.82, 38.63 and 45.34 MeV.

There are two reasons why an exact FR analysis which includes the D-state of the deuteron is of interest. Firstly

both groups found that ZR calculations using elastic scattering parameters for the deuteron optical potential give very poor fits to the (p,d) cross section data and also Johnson and Santos[77]) on the basis of approximate calculations expect large effects due to the deuteron D-state in these two transitions. The ZR analysis of Chant et al[72]) led to good descriptions of the cross-section data using an "adjusted deuteron potential". This potential is based upon an elastic scattering parameter set[78]) and differs essentially in using a much larger surface absorption. Table 4.3 gives the optical parameters used in the present calculations. Set B is the "adjusted deuteron potential" of ref.[72]) which is used for both levels despite the 7 MeV difference between the respective energies of the outgoing deuteron as shown in table 4.4. The proton potential is based on the formula of ref.[74]) extrapolated to the elastic scattering of protons by ^{16}O. The neutron parameters are consistent with the previous calculations but differ from those of ref.[76]).

Fig. 4.7(a) shows the ZR predictions and exact FR calculations with and without the D-state. The values of D_0^2 and the spectroscopic factors (ideally expected to be 2 for the g.s. and 4 for the 6.18 MeV state[76])) are given in table 4.4. It is seen that the D-state has significantly affected the cross section shape and increased the magnitude of the first peak by ~5 and ~23 percent for the $J = \frac{1}{2}$ and $\frac{3}{2}$ levels, respectively. While these adjusted deuteron parameters reproduce the shapes of the cross sections satisfactorily the corresponding spectroscopic factors

Table 4.3

POTENTIALS FOR $^{16}O(p,d)^{15}O$

	Deuteron			Proton[d] Ep(MeV)			Neutron
	A[a]	B[b]	C[c]	25.52	30	31.82	
V (MeV)	118	114.2	100.33	47.1	46.94	45.09	adjusted
r_V (fm)	0.934	0.92	0.99	1.17	1.17	1.17	1.25
a_V (fm)	0.792	0.84	0.78	0.75	0.75	0.75	0.65
W_V (MeV)				2.91	3.9	4.3	
W (MeV)	5.95	32.6	7	5.42	4.3	3.85	
r_W (fm)	1.58	1.58	1.545	1.32	1.32	1.32	
a_W (fm)	0.777	0.53	0.7	0.51	0.51	0.51	
S (MeVfm^2)	12	12	13.5	12.4	12.4	12.4	
r_s (fm)	0.934	0.92	0.99	1.01	1.01	1.01	
a_s (fm)	0.792	0.84	0.78	0.75	0.75	0.75	

r_c = 1.3 fm

a) ref.[80] b) ref.[72] c) see text d) ref.[74]

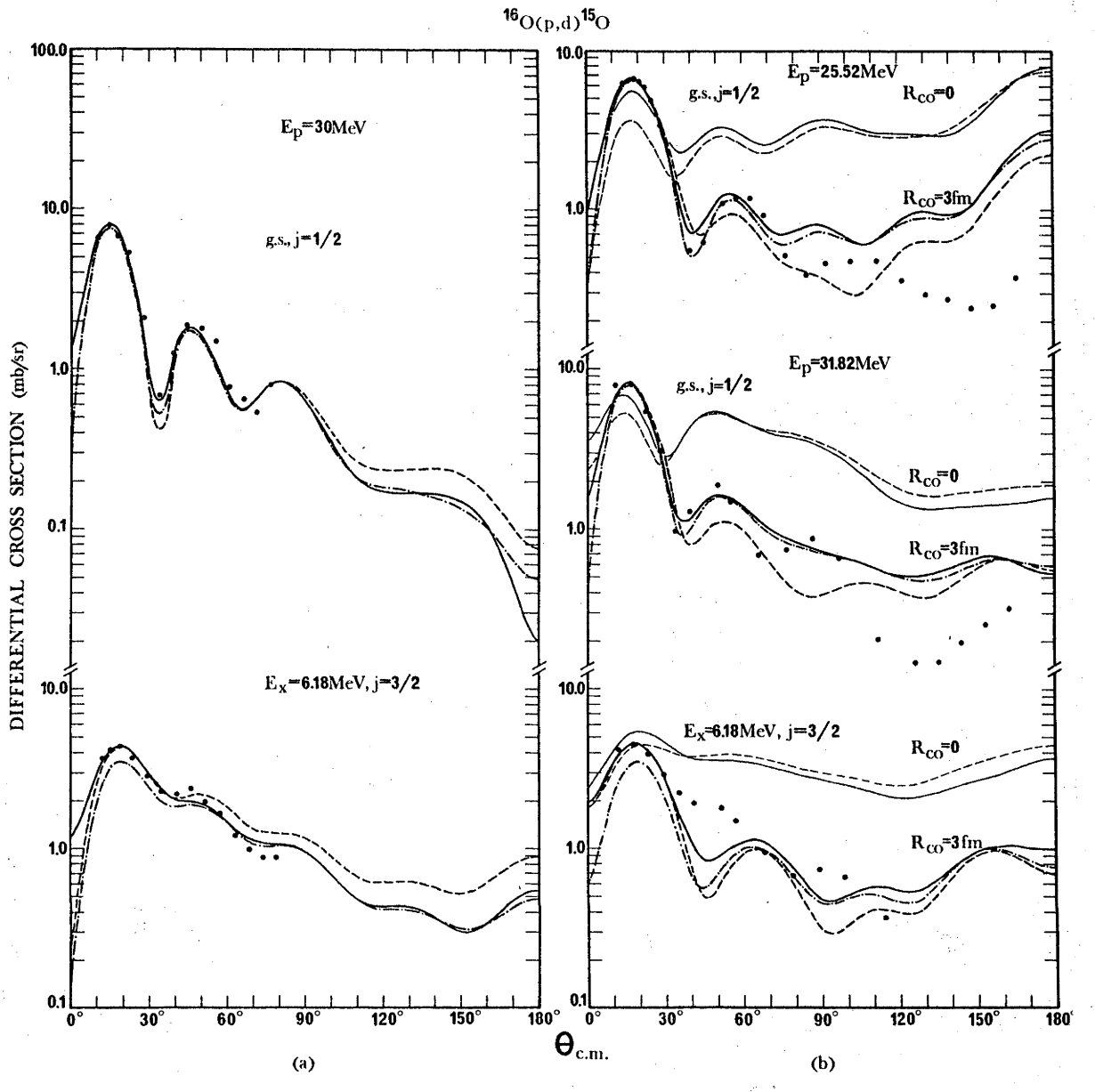

Fig. 4.7. Differential cross sections for the reaction $^{16}O(p,d)^{15}O$ leading to the g.s. $\left(\frac{1}{2}^-\right)$ and 6.18 MeV $\left(\frac{3}{2}^-\right)$ level in ^{15}O at 25.52, 30 and 31.82 MeV proton bombarding energies. The solid and dash-dot curves are the exact FR calculations with and without the D-state respectively and the broken curves the ZR predictions for the parameters of Table 4.3 (see also Table 4.4). In (b) the FR S+D and ZR calculations with a lower radial cut-off at 3 fm (R_{co} = 3 fm) are normalized to the data at the first peak and the corresponding calculations without a cut-off (R_{co} = 0) show the relative difference in magnitude at the first peak. The data are those of ref.[72,76]).

Table 4.4[a])

DEUTERON ENERGIES, D_0^2 AND SPECTROSCOPIC FACTORS FOR $^{16}O(p,d)^{15}O$

E_p (MeV)	Q (MeV)	E_d [b]) (MeV)	D_0^2 (10^4MeV^{2}fm^3)	σ_{expt} (mb/sr)	σ_{th}(FRS+D) (mb/sr)	σ_{th}(ZR)[c]) (mb/sr)	S(FRS+D)	S(ZR)[c])
30	-13.44	16.8B	1.24	7.96	1.31	1.74	6.08	4.58
	-19.62	9.8B	1.41	4.40	0.23	0.27	19.13	16.30
25.52	-13.44	12A	1.56(1.05)	6.78	1.58(1.90)	1.68(2.99)	4.29(3.57)	4.04(2.27)
31.82	-13.44	18.7C	1.41(1.10)	8.19	3.14(3.70)	3.66(5.54)	2.61(2.21)	2.24(1.48)
	-19.62	11.7A	1.45(1.21)	4.52	1.33(1.11)	1.51(1.52)	3.40(4.07)	2.99(2.97)

a) numbers in parentheses correspond to calculations with R_{co} = 3 fm.

b) letters refer to deuteron parameter set used (see table 4.3).

c) using $D_0^2 = 1.65 \times 10^4$MeV^{2}fm^3.

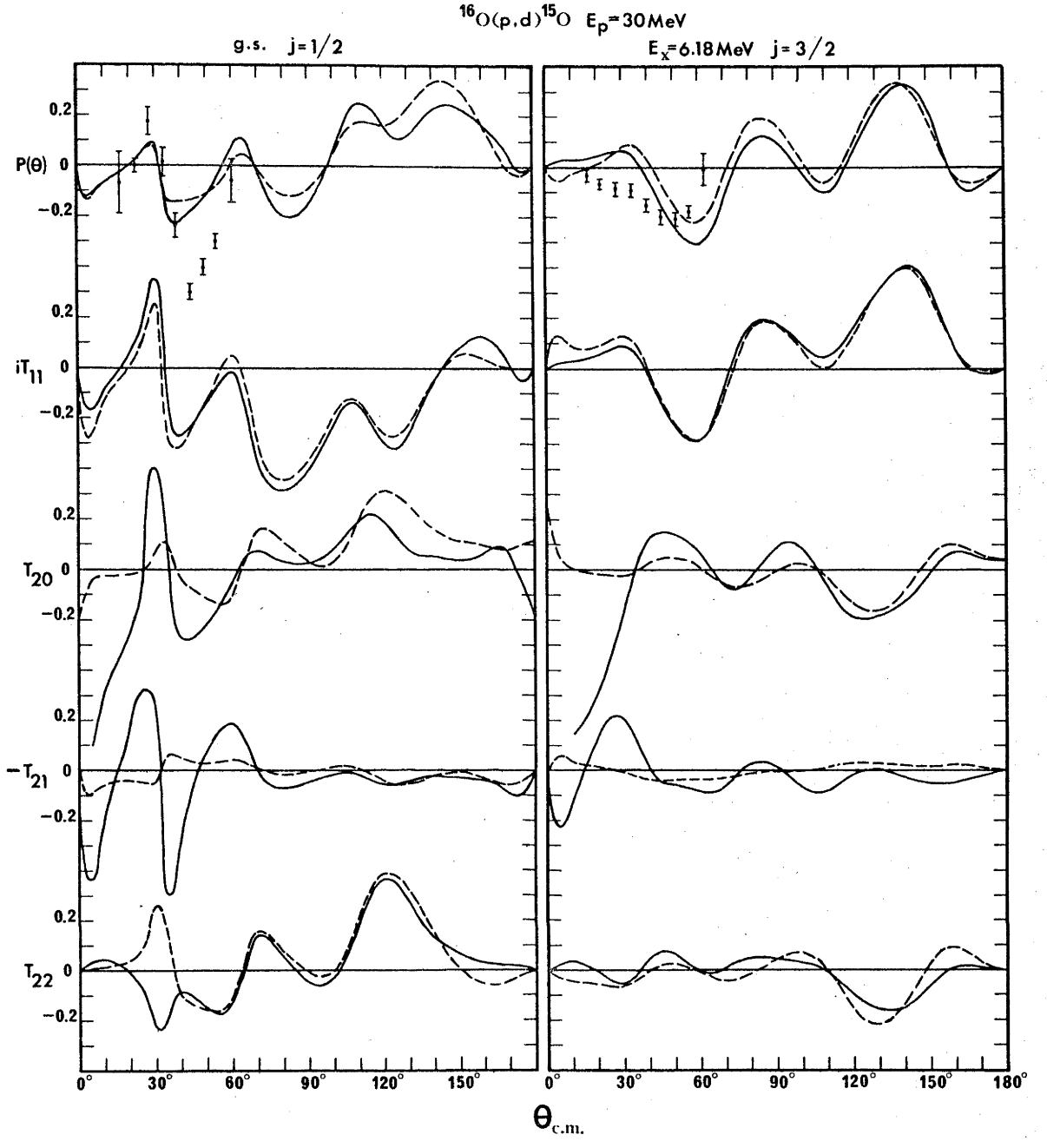

Fig. 4.8. Proton analysing powers and deuteron polarizations for the reaction $^{16}O(p,d)^{15}O$ (g.s. and 6.18 MeV level) at 30 MeV bombarding energy. The solid and broken curves are the exact FR S+D-state and ZR predictions respectively for the parameters of Table 4.3 (see also Table 4.4). The points are the data of ref.[72]).

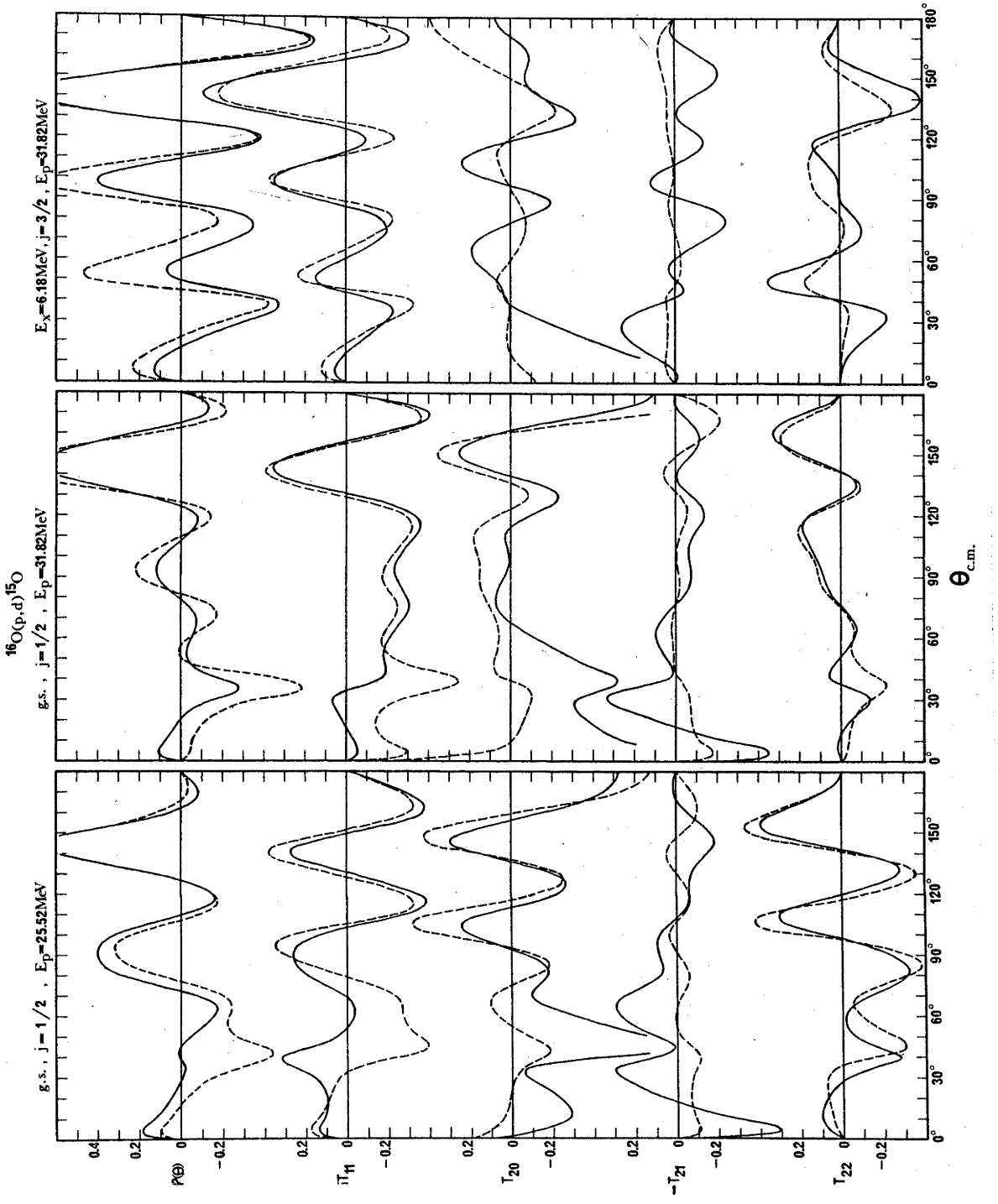

Fig. 4.9. Proton analysing powers and deuteron polarizations for the reaction $^{16}O(p,d)^{15}O$ (g.s. and 6.18 MeV level) at 25.52 and 31.82 MeV bombarding energies. The solid and broken curves are the exact FR S+D-state and ZR predictions respectively for the parameters of Table 4.3 (see also Table 4.4) and a lower radial cut-off at 3 fm.

are inadequate. The spectroscopic factors depend on the choice of the neutron form factor[57]). In the ZR calculation for the $J = \frac{1}{2}$ level for example, a 4 percent reduction of the neutron real well radius produced a decrease of ~12 percent in the magnitude of the first peak and vice-versa[50]). Fig. 4.8 shows the corresponding proton analysing powers $P(\theta)$ and deuteron vector polarizations $\langle iT_{11} \rangle$ and tensor polarizations $\langle T_{2k} \rangle$. The FR S-state calculations which are not shown, differ significantly from the corresponding ZR predictions for $P(\theta)$ and $\langle iT_{11} \rangle$ but for the $\langle T_{2k} \rangle$ the two calculations are similar and practically identical at forward angles. Thus the large effects on the $\langle T_{2k} \rangle$ for both j-values in the region 0 to 60^0 are due to the inclusion of the deuteron D-state in the exact FR treatment. The data for the analysing powers $P(\theta)$ are from ref.[72]) and the improvement in fit over that analysis even in ZR can only be due to the use of different proton parameters. Recent work on deuteron elastic scattering by ^{16}O (ref.[79])) and ^{24}Mg (ref.[69])) has shown that improved fits to the deuteron tensor polarizations are obtained at forward angles when a small T_R tensor term[2,53]) with a preferred form factor of the Woods-Saxon derivative type[69]) is included in the deuteron-nucleus optical potential. The present FR S+D-state calculations were repeated with a small T_R tensor included with $M = -0.5$ MeV, $r_R = 2.5$ fm and $a_R = 2.5$ fm[69,79]). Significant effects were found for the deuteron tensor polarizations where the D-state effects were slightly enhanced.

In their ZR analysis Snelgrove and Kashy[76]) in an attempt

to extract reasonable spectroscopic factors while using elastic scattering OM parameters were led to the use of a lower radial cut-off at 3 fm. In the present work similar ZR and FR calculations are reported for the g.s. J = ½ level at proton bombarding energies of 25.52 and 31.82 MeV and the 6.18 MeV, J = ³⁄₂ level at 31.82 MeV. Table 4.4 gives the outgoing deuteron energies corresponding to the proton bombarding energies for each level and indicates which deuteron parameter set of table 4.3 was used in the respective calculations. Parameter set A is the result of an analysis of deuteron elastic scattering by ^{16}O at 11.8 MeV bombarding energy[80]). Parameter set C at 19 MeV was derived from analyses at 16.3 MeV (ref.[78])), 34.4 MeV (ref.[81])) and 52 MeV (ref.[82])) and is similar to that used by Snelgrove and Kashy. The elastic scattering analyses indicated that a spin-orbit term in the potential was necessary although its strength is poorly determined[80,82]). Thus in view of the similarity of the imaginary potentials, parameter sets A and C differ essentially in the real part of the deuteron potential. Analyses of proton elastic scattering by ^{16}O in the region of 30 MeV have consistently given poor fits to the data at backward angles[76,83-85]). The most recent and detailed analysis by van Oers and Cameron[86]) encountered the same difficulties which were traced to the presence of several wide resonances[87]) in the energy range 20-30 MeV. In the ZR 30 MeV calculations (see fig. 4.8) the extrapolation of the "optimum proton-nucleus standard OM parameters" formula of ref.[74]) to proton scattering by ^{16}O gave an improved theoretical fit to the proton analysing powers P(θ) compared with an analysis[72]) which

used the elastic scattering parameters of Barrett et al[84]). This extrapolation was used in the present calculations and the resulting parameters which do not differ greatly from those of ref.[76]) are given in table 4.3. Fig. 4.7(b) shows the ZR, FR S-state and FR S+D-state calculations using a lower radial cut-off at 3 fm (R_{CO} = 3 fm) for the J = $\frac{1}{2}$ level at 25.52 and 31.82 MeV and the J = $\frac{3}{2}$ level at 31.82 MeV. These calculations were normalized by the procedure described in section 4.3 and the corresponding results with R_{CO} = 0 are included to show the relative difference in magnitude at the first peak. This shows clearly that for the J = $\frac{1}{2}$ level at the two energies, the magnitude of the first peak is increased to a much greater extent by introducing a 3 fm cut-off in the ZR calculation than it is in the FR S+D-state treatment. For the J = $\frac{3}{2}$ level in ZR a 3 fm cut-off has only a very small effect on the magnitude of the first peak while in the corresponding FR S+D-state calculation it leads to a significant reduction. When both R_{CO} = 3 fm calculations are normalized at the first peak the FR S+D-state curve no longer lies below the corresponding ZR result at large angles. Table 4.4 summarizes the values of D_0^2 and the spectroscopic factors for these calculations. Introduction of a cut-off in the FR S+D-state calculation gives a good description of the shape and relative magnitudes of the first and second peak for the J = $\frac{1}{2}$ level at both energies with some improvement for the J = $\frac{3}{2}$ level but the fits at backward angles are unsatisfactory. The effects of the deuteron D-state on the cross sections still persist despite the use of a cut-off, particularly the 28 percent increase in magnitude of the

first peak for the J = $\frac{3}{2}$ level. Fig. 4.9 shows the proton analysing powers P(θ), deuteron vector polarizations $\langle iT_{11} \rangle$ and tensor polarizations $\langle T_{2k} \rangle$ for ZR and FR S+D-state calculations with a lower radial cut-off at 3 fm. For P(θ) and $\langle iT_{11} \rangle$ the differences between the FR S-state and the ZR calculations are now quite significant (as are the effects of the D-state particularly at forward angles). In the case of $\langle T_{21} \rangle$ (and in general $\langle T_{20} \rangle$ and $\langle T_{22} \rangle$ at forward angles) the ZR and FR S-state calculations are very similar. Therefore the large differences between the FR S+D-state and ZR calculations are due mainly to the deuteron D-state and not the FR interaction.

4.5 Conclusions

For the two ℓ = 1 transitions studied in the reaction $^{52}Cr(d,p)^{53}Cr$ the shapes (and hence the j-dependent effects) of the angular distributions and vector analysing powers were insignificantly altered by including the D-state of the deuteron in an exact FR DWBA calculation. However, the corresponding tensor analysing powers, especially $\langle T_{20} \rangle$ and $\langle T_{21} \rangle$ (which is very small at forward angles in ZR) were considerably changed. The ZR constant D_0^2 was found to be 1.42 and 1.46 × 10^4 MeV^2 fm^3, respectively, for the transitions to the ground ($\frac{3}{2}^-$) and 0.57 MeV ($\frac{1}{2}^-$) states.

The inclusion in the D-state FR calculations of a small T_R tensor term in the deuteron optical potential caused significant changes in the tensor analysing powers $\langle T_{20} \rangle$ and $\langle T_{21} \rangle$ but

left the corresponding angular distributions, vector analysing powers and tensor analysing powers $\langle T_{22} \rangle$ largely unaffected.

Calculations in the exact FR treatment for two $\ell = 1$ transitions in the reaction $^{40}Ca(d,p)^{41}Ca$ leading to the 2.47 ($\frac{3}{2}^-$) and 3.95 MeV ($\frac{1}{2}^-$) levels at 7 to 12 MeV deuteron bombarding energy showed (similar to the results of the previous cases) that j-dependent effects in the cross section, proton polarization and deuteron vector analysing power were negligibly altered by the inclusion of the deuteron D-state. Elastic scattering OM parameters led to good fits to the data for the (d,p) cross sections and corresponding deuteron vector analysing powers. The FR S+D-predictions indicated that the FR correction factor is $\sim 1.44 \times 10^4$ MeV^2 fm^3, in agreement with the result for $^{52}Cr(d,p)$. The deuteron tensor analysing powers $\langle T_{20} \rangle$, $\langle T_{21} \rangle$ (which is vanishingly small at forward angles in ZR) and to a lesser extent $\langle T_{22} \rangle$ for both j-values showed significant differences due to the inclusion of the deuteron D-state. There was no obvious trend of the D-state effect either as a function of energy or OM parameters in any of these quantities.

Exact FR calculations using adjusted deuteron parameters for two $\ell = 1$ transitions in the reaction $^{16}O(p,d)^{15}O$ leading to the g.s. ($\frac{1}{2}^-$) and the 6.18 MeV ($\frac{3}{2}^-$) level at an incident proton energy of 30 MeV show that the cross sections are significantly modified by the inclusion of the deuteron D-state. Consistent with the result for $^{40}Ca(d,p)$ and $^{52}Cr(d,p)$ the FR S+D-state

calculations lie below the ZR predictions at large angles. The deuteron vector polarizations and proton analysing powers were also significantly altered, while the corresponding deuteron tensor polarizations $\langle T_{20} \rangle$ and $\langle T_{21} \rangle$ (and to a lesser extent $\langle T_{22} \rangle$) showed very large effects at forward angles. Calculations with a small T_R tensor term in the deuteron-nucleus optical potential produced small effects by comparison with those due to the D-state. For the same transitions at E_p = 25.52 and 31.82 MeV the FR S+D-state calculations using elastic scattering deuteron parameters with an artificial lower radial cut-off at 3 fm gave reasonable spectroscopic factors and satisfactory fits to the cross section data only at forward angles. The introduction of a cut-off did not reduce the effects due to the inclusion of the deuteron D-state.

CHAPTER 5

DISCUSSION AND SUMMARY

Discussion

Deuteron elastic scattering is essentially dependent upon the asymptotic form of the distorted waves[78,88]. Thus the OM parameters determined from an elastic scattering analysis are those which optimize the wave functions in this region. For the corresponding reaction, the calculation of the transition matrix amplitudes involves integration over these deuteron wave functions for all values of the radial coordinate. The calculations in chapter 4 using a lower radial cut-off at 3 fm in this integration indicated that there was a significant contribution from the nuclear interior. Thus the determination of the exact form of the deuteron radial wave functions in the nuclear interior and surface region is of importance. It is not clear that the OM produces the correct functional form of the deuteron distorted waves in the region of the nuclear surface, even while it does so asymptotically. The OM does not account for the strong distortion and probable break-up that the deuteron experiences in the nuclear surface region and furthermore, it is unlikely that the deuteron retains its identity in the interior of the nucleus. Consequently the exact form of the deuteron wave function in the nuclear interior is not clear. Thus it is to be expected that different parameters (see chapter 2) may be required to describe elastic scattering and reaction data. This was the result of a

quantitative study by Baz' et al[65]) who concluded that "the optical model and the method of distorted waves are just heuristic methods, where the optical potential parameters [for the deuteron] have no great physical significance". The use of different parameters may be interpreted as compensating in part, for the inadequacies of the models used. However, it is interesting to note that the elastic parameters discussed in chapter 2 were the result of an analysis of elastic cross-section data only, while those used in chapter 4 for the $^{40}Ca(d,p)^{41}Ca$ reaction at 7 MeV (see fig. 4.4) resulted from an extensive elastic scattering analysis[52]) which included vector polarization data as well, and also comparison with tensor polarizations. Such a comprehensive elastic scattering analysis may possibly do more to specify the details of the OM potential.

An alternative approach to using the deuteron centre-of-mass - nucleus optical potential[89]) is to treat separately the nucleon-nucleus potentials of the two nucleons in the deuteron without actually solving (as is done by Shanely and Aaron[90]) for example) a three body problem. Johnson et al[59,91]) used deuteron distorted waves generated by an "adiabatic potential" which was determined from the effective two body potentials of the nucleon-target interactions. These interactions were taken to be optical potentials evaluated at half the incident deuteron energy. Consideration of channels involving ^3S states of the neutron-proton system and the ground state of the target nucleus led to a straightforward modification of the usual DW method. The

distorted waves obtained in this manner contained contributions due to deuteron break-up in the region of the nuclear field. The results of ref.[91]) indicated that such distorted waves may have a more satisfactory functional form in the nuclear surface region than do the conventional OM wave functions of the DWBA. In this adiabatic treatment however, it was found that while the ambiguity associated with the deuteron OM potential was eliminated, the final results were dependent on the choice of nucleon optical potentials and this dependence in turn was related to the strong L-space localization[92]) inherent in this theory.

Some recent studies by various workers[57,93-96]) indicated that the use of single particle form factors for the transferred neutron in deuteron or proton induced reactions may not be adequate. This assumption and the lack of a proper treatment of inelastic effects may be a partial explanation of the difficulties encountered for the two transitions studied in chapter 4 for $^{16}O(p,d)^{15}O$.

Summary

In conclusion a brief summary is made of some of the main points of the thesis.

Using the DWBA theory and the OM, satisfactory agreement with experiment can be obtained in the description of j-dependent features of the cross section and deuteron vector analysing power for $\ell = 1$ transitions in $^{50,52}Cr(d,p)$ and $^{40}Ca(d,p)$ reactions. In some cases a variation in parameters away from the elastic

scattering results was necessary to achieve this agreement*). For these reactions the introduction of a FR interaction led to only slight modifications of the cross section shape and deuteron vector and tensor analysing powers, while the inclusion of the deuteron D-state in the FR calculation caused significant changes in the deuteron tensor analysing powers. Comparison of cross sections for ZR and FR calculations gave a value of ~1.44 × 10^4 MeV^2 fm^3 for D_0^2, the FR correction factor. This value is smaller than has been usually assumed[21]). A study of two possible tensor interactions in the deuteron-nucleus OM potential indicated a preference for the T_R potential. This tensor potential led to significant modifications of the deuteron tensor analysing powers, but these modifications were generally less than those due to the inclusion of the deuteron D-state. Within the limitations of the OM and DWBA, large effects due to the deuteron D-state were predicted (particularly for the tensor polarizations) for the two ℓ = 1 transitions studied in the $^{16}O(p,d)^{15}O$ reaction. The calculations with a lower radial cut-off (see fig. 4.7(b)) confirmed that in the FR treatment, contributions from the nuclear interior, while still important, are of less significance than they are in ZR.

---

*) Calculations performed by Dr. B.A. Robson (unpublished) have shown that the description of elastic scattering cross section and polarization data for $^{40}Ca(d,d)$ is practically insensitive to the magnitude of the deuteron spin-orbit radius in the range 0.78-1.10fm. These two extreme values for the deuteron spin-orbit radius were used in calculations for ℓ=1 transitions in the reaction $^{40}Ca(d,p)^{41}Ca$ and the results indicated that, while the j-dependence of the cross sections was evident in both cases, the smaller radius is preferable.

APPENDIX

a) The Jacobian for a transformation of variables of integration from $\underline{r}$ and $\underline{r}'$ to $\underline{r}_1$ and $\underline{r}_2$ where

$$\underline{r} = a\underline{r}_1 + b\underline{r}_2$$

and $$\underline{r}' = a'\underline{r}_1 + b'\underline{r}_2$$

is given by $(ab' - a'b)^3$ since

$$J_x = \begin{vmatrix} \frac{\partial x}{\partial x_1} & \frac{\partial x}{\partial x_2} \\ \frac{\partial x'}{\partial x_1} & \frac{\partial x'}{\partial x_2} \end{vmatrix} = ab' - a'b, \text{ etc.}$$

and $$J = J_x \cdot J_y \cdot J_z$$

In this case (for the vector diagram of fig. A.1)

$$\underline{r}_{pR} = \underline{r}_{pR} \tag{A.1}$$

$$\underline{r}_{nT} = -\frac{m_p}{m_p + m_n}\,\underline{r}_d + \underline{r}_{dT} \tag{A.2}$$

and $$\underline{r}_d = \underline{r}_{pR} - \frac{M_T}{M_T + m_n}\,\underline{r}_{nT} \tag{A.3}$$

substituting eqn. (A.3) into eqn. (A.2) gives

$$\underline{r}_{nT} = \left(1 - \left[\frac{m_p}{m_p+m_n}\right]\left[\frac{M_T}{M_T+m_n}\right]\right)^{-1}\left(-\left[\frac{m_p}{m_p+m_n}\right]\underline{r}_{pR} + \underline{r}_{dT}\right) \tag{A.4}$$

from eqn. (A.1): $a = 1$

$b = 0$

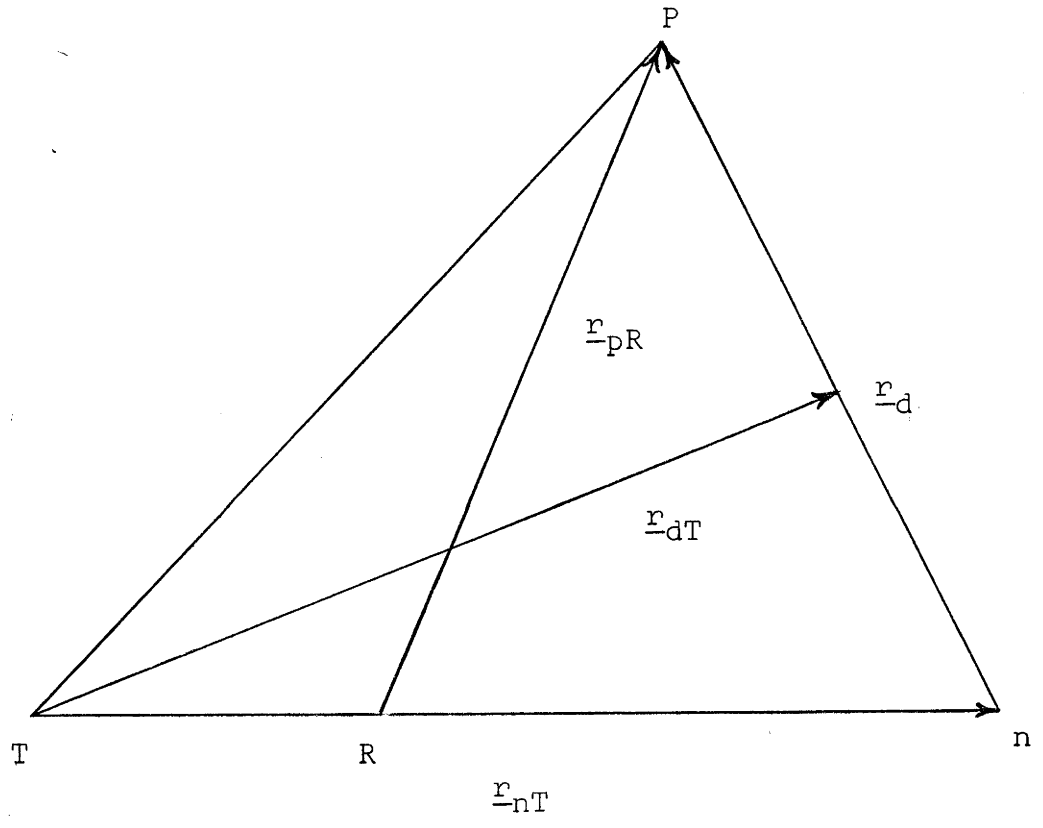

Fig. A.1 Coordinate vectors for the reaction T(d,p)R

from eqn. (A.4): $$a' = -\left(\left[\frac{m_p}{m_p+m_n}\right]^{-1} - \left[\frac{M_T}{M_T+m_n}\right]\right)^{-1}$$

$$b' = \left(1 - \left[\frac{m_p}{m_p+m_n}\right]\left[\frac{M_T}{M_T+m_n}\right]\right)^{-1}$$

b) It is possible to write $\underline{r}_{nT}$ and $\underline{r}_d$ as linear combinations of $\underline{r}_{pR}$ and $\underline{r}_{dT}$:

$$\underline{r}_{nT} = s_1 \underline{r}_{pR} + t_1 \underline{r}_{dT} \tag{A.5}$$

$$\underline{r}_d = s_2 \underline{r}_{pR} + t_2 \underline{r}_{dT} \tag{A.6}$$

then from eqn. (A.4)

$$s_1 = -\frac{m_p(M_T+m_n)}{m_n(M_T+m_p+m_n)}$$

$$t_1 = \frac{(m_p+m_n)(M_T+m_n)}{m_n(M_T+m_p+m_n)}$$

Substituting eqn. (A.5) into eqn. (A.3) gives

$$s_2 = t_1$$

$$t_2 = -\frac{M_T(m_n+m_p)}{m_n(M_T+m_n+m_p)}$$

In the calculations it is assumed that

$$m_p + m_n = m_d$$

$$M_T + m_n = M_R$$

whence

$$s_1 = -\frac{m_p M_R}{m_n(M_T+m_d)}$$

$$t_1 = s_2 = \frac{m_d M_R}{m_n(M_T+m_d)}$$

$$t_2 = -\frac{M_T m_d}{m_n(M_T+m_d)}$$

REFERENCES

[1]) W. Tobochman, Theory of direct nuclear reactions (Oxford University Press, 1961).

[2]) G.R. Satchler, Nucl.Phys. 21 (1960) 116.

[3]) W. Tobocman, Phys.Rev. 115 (1959) 98.

[4]) L.L. Lee, J.P. Schiffer, B. Zeidman, G.R. Satchler, R.M. Drisko and R.H. Bassel, Phys.Rev. 136 (1964) B971; Errata, Phys.Rev. 138 (1965) 7AB6.

[5]) R.M. Drisko and G.R. Satchler, Phys.Lett. 9 (1964) 342.

[6]) J.R. Mines, Nucl.Phys. 86 (1966) 89.

[7]) P.J.A. Buttle and L.J.B. Goldfarb, Proc.Phys.Soc. 83 (1964) 701.

[8]) Gy. Bencze and J. Zimanyi, Phys.Lett. 9 (1964) 246.

[9]) F.G. Perey and D. Saxon, Phys.Lett. 10 (1964) 107.

[10]) R.C. Johnson and F.D. Santos, Phys.Rev.Lett. 19 (1967) 364.

[11]) R.C. Johnson, Nucl.Phys. A90 (1967) 289.

[12]) C.A. Pearson, D. Rickel and D. Zissermann, Nucl.Phys.A148 (1970) 273.

[13]) C.A. Pearson and D. Zisserman, Nucl.Phys. A154 (1970) 23.

[14]) R.V. Reid, Ann. of Phys. 50 (1968) 411.

[15]) G.R. Satchler, Nucl.Phys. 55, (1964) 1.

[16]) B.A. Robson, An introduction to scattering theory and direct reactions (a series of lectures given at the I.A.S. of the Aust.Nat.Univ.) ANU P/351, 2nd ed.

[17]) D. Robson, Nucl.Phys. 22 (1961) 34, 47.

[18]) N.F. Mott and H.S.W. Massey, The theory of atomic collisions, 3rd ed. (Clarendon Press, Oxford, 1965).

[19]) M.E. Rose, Elementary theory of angular momentum, (Wiley, New York, 1957).

[20]) R. Huby, M.Y. Refai and G.R. Satchler, Nucl.Phys. 9 (1958/9) 94.

[21]) G.R. Satchler, Lectures in theoretical physics, vol.VIII-C (University of Colorado Press, Boulder, 1965) 122.

[22]) D. Brink and G.R. Satchler, Angular momentum, 2nd ed. (Clarendon Press, Oxford, 1968).

[23]) B.A. Robson, A Fortran program for elastic deuteron scattering, Oak Ridge Nat.Lab. ORNL-TM1831 (1967).

[24]) B.A. Robson, Lectures on scattering and polarization of nucleons and deuterons (given at the I.A.S. of the Aust.Nat. Univ.) ANU P/497.

[25]) S. Devons and L.J.B. Goldfarb, Handbuch der Physik, ed. S. Flügge, vol.XLII, 362 (Springer-Verlag, Berlin, 1957).

[26]) U. Fano, Rev.Mod.Phys. 29 (1957) 74.

[27]) L.J.B. Goldfarb, Nucl.Phys. 7 (1958) 622.

[28]) G.R. Satchler, Nucl.Phys. 8 (1958) 65.

[29]) W. Lakin, Phys.Rev. 98 (1955) 139

[30] N. Austern, R.M. Drisko, E.C. Halbert and G.R. Satchler, Phys.Rev. 133 (1964) B3.

[31] M. Moshinsky, Nucl.Phys. 13 (1959) 104.

[32] I.N. Sneddon, Special functions of mathematical physics and chemistry, 2nd ed. (Oliver and Boyd, Edinburgh, 1961).

[33] P.T. Andrews, R.W. Clifft, L.L. Green and J.F. Sharpey-Schafer, Nucl.Phys. 56, (1964) 465.

[34] M.N. Rao, J. Rapaport, A. Sperduto and D.L. Smith, Nucl.Phys. A121, (1968) 1.

[35] R. Bock, H.H. Duhm, S. Martin, R. Rüdel and R. Stock, Nucl. Phys. 72 (1965) 273.

[36] T.J. Yule and W. Haeberli, Nucl.Phys. A117 (1968) 1.

[37] T.J. Yule and W. Haeberli, Phys.Rev.Lett. 19 (1967) 756.

[38] P.J. Bjorkholm, W. Haeberli and B. Mayer, Phys.Rev.Lett. 22 (1969) 955.

[39] D.C. Kocher and W. Haeberli, Phys.Rev.Lett. 23 (1969) 315, 25 (1970) 36.

[40] P.T. Andrews, R.W. Clifft, L.L. Green and R.N. Maddison, Nucl.Phys. 56 (1964) 422.

[41] L.L. Lee and J.P. Schiffer, Phys.Rev. 154 (1967) 1097.

[42] J.L. Alty, L.L. Green, G.D. Jones and J.F. Sharpey-Schafer, Nucl.Phys. A100 (1967) 191.

[43]) J.E. Robertshaw, S. Mecca, A. Sperduto and W.W. Buechner, Phys.Rev. 170 (1968) 1013.

[44]) D.M. Rosalky, D.J. Baugh, J. Nurzynski and B.A. Robson, Nucl. Phys. A142 (1970) 469.

[45]) L.L. Lee and J.P. Schiffer, Phys.Rev.Lett. 12 (1964) 108.

[46]) L.L. Lee and J.P. Schiffer, Phys.Rev. 136 (1964) B405.

[47]) J.P. Schiffer, L.L. Lee, A. Marinov and C. Mayer-Böricke, phys.Rev. 147 (1966) 829.

[48]) C. Glashausser and M.E. Rickey, Phys.Rev. 154 (1967) 1033.

[49]) D. von Ehrenstein and J.P. Schiffer, Phys.Rev. 164 (1967) 1374.

[50]) K.K. Seth, J. Picard and G.R. Satchler, Nucl.Phys. A140 (1970) 577.

[51]) B.A. Robson, Phys.Lett. 26B (1968) 501.

[52]) P. Schwandt and W. Haeberli, Nucl.Phys. A123 (1969) 401.

[53]) G. Delic and B.A. Robson, Nucl.Phys. A127 (1969) 234.

[54]) G. Delic and B.A. Robson, to be published in Nuclear Physics.

[55]) G. Delic, to be published in Nuclear Physics.

[56]) A. Prakash, Phys.Rev.Lett. 20 (1968) 864.

[57]) R.H. Ibarra and B.F. Bayman, Phys.Rev. C 1 (1970) 1786.

[58]) G.A. Bartholemew, E.D. Earle and M.R. Gunye, Can.J.Phys. 44 (1966) 2111.

[59]) R.C. Johnson and P.J.R. Soper, Phys.Rev.C 1 (1970) 976.

[60]) L.J.B. Goldfarb and R.G. Seyler, Nucl.Phys. A149 (1970) 545.

[61]) K.D. Bowers, Proc.Phys.Soc. A65 (1952) 860.

[62]) D.M. Van Patter, N. Nath, S.M. Malik and M.A. Rothman, Phys. Rev. 128 (1962) 1246.

[63]) G.A. Bartholemew and M.R. Gunye, Can.J.Phys. 43 (1965) 1128.

[64]) V.P. Bochin, K.I. Zherebtsova, V.S. Zolotarev, V.A. Komarov, L.V. Krasnov, V.F. Litvin, Yu.A. Nemilov, B.G. Novatsky and Sh. Piskorzh, Nucl.Phys. 51 (1964) 161.

[65]) A.I. Baz', V.F. Demin, M.V. Zhukov and I.I. Kuz'min, Sov.J. Nucl.Phys. 7 (1968) 346.

[66]) P. Schwandt and W. Haeberli, Nucl.Phys. A110 (1968) 585.

[67]) H. Cords, G.U. Din, M. Ivanovich and B.A. Robson, Nucl.Phys. A113 (1968) 608.

[68]) H. Cords, G.U. Din and B.A. Robson, Nucl.Phys. A127 (1969) 95.

[69]) A. Djaloeis and J. Nurzynski, to be submitted to Nuclear Physics.

[70]) G.R. Satchler, private communication to B.A. Robson.

[71]) R.H. Bassel, R.M. Drisko, G.R. Satchler, L.L. Lee, J.P. Schiffer and B. Zeidman, Phys.Rev. 136 (1964) B960.

[72]) N.S. Chant, P.S. Fisher and D.K. Scott, Nucl.Phys. A99 (1967) 669.

[73]) G. Delic and B.A. Robson, Nucl.Phys. A134 (1969) 470.

[74]) F.D. Becchetti and G.W. Greenlees, Phys.Rev. 182 (1969) 1190.

[75]) C.M. Perey and F.G. Perey, Phys.Rev.132 (1963) 755, 152 (1966) 923.

[76]) J.L. Snelgrove and E. Kashy, Phys.Rev. 187 (1969) 1246; B.M. Preedom, J.L. Snelgrove and E. Kashy, Phys.Rev. C 1 (1970) 1132.

[77]) R.C. Johnson, private communication.

[78]) P.E. Hodgson, Adv. in Phys. 15 (1966) 329.

[79]) H. Cords, G.U. Din and B.A. Robson, Nucl.Phys. A134 (1969) 561.

[80]) W. Fitz, R. Jahr and R. Santo, Nucl.Phys. A101 (1967) 449.

[81]) E. Newman, L.C. Becker and B.M. Preedom, Nucl.Phys. A100 (1967) 225.

[82]) B. Duelli, F. Hinterberger, G. Mairle, U. Schmidt-Rohr, P. Turek and G. Wagner, Phys.Lett. 23 (1966) 485.

[83]) C.C. Kim, S.M. Bunch, D.W. Devins and H.H. Forster, Nucl.Phys. 58 (1964) 32.

[84]) R.C. Barrett, A.D. Hill and P.E. Hodgson, Nucl.Phys. 62 (1965) 133.

[85]) J.A. Fannon, E.J. Burge, D.A. Smith and N.K. Ganguly, Nucl. Phys. A97 (1967) 263.

[86]) W.T.H. van Oers and J.M. Cameron, Phys.Rev. 184 (1969) 1061.

[87]) O. Karban, P.D. Greaves, V. Hnizdo, J. Lowe, N. Berovic, H. Wojciechowski and G.W. Greenlees, Nucl.Phys. A132 (1969) 548.

[88]) P.E. Hodgson, The optical model of elastic scattering, (Clarendon Press, Oxford, 1963).

[89]) S. Watanabe, Nucl.Phys. 8 (1958) 484.

[90]) P.E. Shanley and R. Aaron, Ann. of Phys. 44 (1967) 363.

[91]) J.D. Harvey and R.C. Johnson, to be published.

[92]) M.B. Hooper, Nucl.Phys. 76 (1966) 449.

[93]) N. Austern, Phys.Rev. 136 (1964) B1743.

[94]) W.T. Pinkston and G.R. Satchler, Nucl.Phys. 72 (1965) 641.

[95]) R.J. Philpott, W.T. Pinkston and G.R. Satchler, Nucl.Phys. A119 (1968) 241.

[96]) A. Prakash and N. Austern, Ann. of Phys. 51 (1969) 418.